Biogeographical patterns and environmental controls of phytoplankton communities from contrasting hydrographical zones of the Labrador Sea

Glaucia M. Fragoso*[1], Alex J. Poulton[2], Igor M. Yashayaev[3], Erica J. H. Head[3], Mark Stinchcombe[2], Duncan A. Purdie[1]

1. Ocean and Earth Science, University of Southampton, National Oceanography Centre Southampton, Southampton UK.; 2. Ocean Biogeochemistry and Ecosystems, National Oceanography Centre; 3.Ocean and Ecosystem Science Division, Department of Fisheries and Oceans, Canada, Bedford Institute of Oceanography.

*Corresponding author e-mail: (Glaucia Fragoso, glaucia.fragoso@noc.soton.ac.uk)

Permanent address: Ocean and Earth Science, National Oceanography Centre Southampton, University of Southampton Waterfront Campus, European Way, Southampton SO14 3ZH, United Kingdom.

ABSTRACT

The Labrador Sea is an important oceanic sink for atmospheric CO_2 because of intensive convective mixing during winter and extensive phytoplankton blooms that occur during spring and summer. Therefore, a broad-scale investigation of the responses of phytoplankton community composition to environmental forcing is essential for understanding planktonic food-web organization and biogeochemical functioning in the Labrador Sea. Here, we investigated the phytoplankton community structure (> 4μm) from near surface blooms (< 50 m) from spring and early summer (2011 to 2014) in detail, including species composition and environmental controls. Spring blooms (> 1.2 mg chl*a* m^{-3}) occurred on and near the shelves in May and in offshore waters of the central Labrador Sea in June due to haline- and thermal-stratification, respectively. Sea ice-related (*Fragilariopsis cylindrus* and *F. oceanica*) and Arctic diatoms (*Fossula arctica*, *Bacterosira bathyomphala* and *Thalassiosira hyalina*) dominated the relatively cold (< 0°C) and fresh (salinity < 33) waters over the Labrador shelf (e.g., on the southwestern side of the Labrador Sea), where sea-ice melt and Arctic outflow predominates. On the northeastern side of the Labrador Sea, intense blooms of the colonial prymnesiophyte *Phaeocystis pouchetii* and diatoms, such as *Thalassiosira nordenskioeldii*, *Pseudo-nitzschia granii* and *Chaetoceros socialis*, occurred in the lower nutrient waters (nitrate < 3.6 μM) of the West Greenland Current. The central Labrador Sea bloom occurred later in the season (June) and was dominated by Atlantic diatoms, such as *Ephemera planamembranacea* and *Fragilariopsis atlantica.* The data presented here demonstrate that the Labrador Sea spring and early summer blooms are composed of contrasting phytoplankton communities, for which taxonomic segregation appears to be controlled by the physical and biogeochemical characteristics of the dominant water masses present.

Keywords: phytoplankton community structure; diatoms; Labrador Sea; *Phaeocystis pouchetii*; stratification; water masses.

1. Introduction

Marine phytoplankton communities respond rapidly (days to weeks) to changes occurring in their physical environment due to their short generation times. Over the last few decades climate change has led to marked physical changes in the Arctic Ocean and adjacent sub-Arctic seas (Yashayaev et al., 2015) – changes which are likely to be reflected by responses in their phytoplankton communities (Anisimov et al., 2007). Climate-driven processes modify the major factors, such as light availability, nutrient input and grazing pressure that shape phytoplankton physiological traits and alter community structure (Montes-Hugo et al., 2009; Litchman et al., 2012). As the climate changes in these high latitude oceans, the parameters that define the phytoplankton phenology (seasonal and interannual variation), biomass, primary production and community structure, will all likely be modified. Alteration of the phytoplankton community propagates into marine food web dynamics and biogeochemical cycles (Finkel et al., 2010), due to traits regarding palatability, cell size, elemental stoichiometry and efficiency of carbon transport to deeper waters. A further advance in understanding the long-term responses of Arctic phytoplankton to climate change can be achieved from remote-sensing-derived observations (e.g., Arrigo et al., 2008; Pabi et al., 2008; Kahru et al., 2011; Ardyna et al., 2014) and *in situ* long-term monitoring (Head et al., 2003; Yashayaev, 2007; Yashayaev et al., 2015).

The Labrador Sea is a sub-Arctic region of the Northwest Atlantic located between Greenland and the eastern coast of Canada. In spite of its small size (< 1% of the Atlantic Ocean), the Labrador Sea plays a critical role in the marine carbon cycle because it is one of the most productive regions of the North Atlantic, which enhances the flux of atmospheric CO_2 into surface waters (DeGrandpre et al., 2006; Martz et al., 2009). Moreover, the

Labrador Sea produces the densest of all water masses that are entirely formed in the subpolar North Atlantic (Yashayaev et al., 2015), where wintertime cooling and wind forcing cause convective sinking of dense surface water, transporting carbon rapidly to the deep ocean (Tian et al., 2004). The Labrador Sea is also a region susceptible to climate change because it receives the discharge of Arctic ice-melt waters, which potentially increases the freshening of surface layers (Dickson et al., 2002; Yashayaev and Seidov, 2015). Due to its biogeochemical significance and potential vulnerability to climate change, a comprehensive understanding of the current phytoplankton communities in the Labrador Sea is crucial to detect climate change effects in the future.

The Labrador Sea is usually characterised by three distinct phytoplankton bloom regions during spring and early summer (Frajka-Williams et al., 2009, Frajka-Williams and Rhines, 2010). In contrast to the south to north progression observed in other regions of the North Atlantic (Henson et al., 2009), the northern bloom (north of 60ºN, in the eastern Labrador Sea) is more intense (satellite-derived chlorophyll (1998-2006) up to 5.5 mg chl*a* m^{-3}, Harrison et al., 2013) and starts early in the season (late April). This is due to the early onset of haline-driven stratification formed by freshwater input from the West Greenland Current (Stuart et al., 2000; Frajka-Williams and Rhines, 2010; Harrison et al., 2013; Lacour et al., 2015). The western bloom located on the Labrador Shelf varies inter-annually, since it is triggered by the rapid melting of sea ice that often covers the shelf well into spring (Wu et al., 2007). The Labrador Shelf bloom development starts as the ice retreats, which is usually in May, although it may occur later (June) in some years (Head et al., 2013). The central Labrador bloom is weaker (1998-2006 satellite-derived chlorophyll < 2 mg chl*a* m^{-3}, Harrison et al., 2013) and occurs later in the season (June) as a result of thermal stratification (Frajka-Williams and Rhines, 2010). Nutrient replenishment, occurring during deep winter mixing (200 – 2300 m) and dependent on cumulative surface heat loss, (Yashayaev and

Loder, 2009), supports the phytoplankton spring bloom once light becomes available (Harrison et al., 2013). Storm events (Wu et al., 2008) as well as upwelling events from cyclonic eddies (Yebra et al., 2009) and glacial meltwater (Bhatia et al., 2013) have all been suggested to sustain the blooms via nutrient replenishment after these are exhausted in surface waters.

The Labrador Sea acts as a receiving and blending basin for Atlantic and Arctic waters (Yashayaev et al., 2015) and, therefore, is an ideal region to study the influence of the environmental factors that shape the phytoplankton community structure due to the Atlantic and Arctic waters that divide the region into distinct hydrographic zones (Head et al., 2000, 2003). Hydrographic zones create ecological niches, where distinct phytoplankton communities occur (Acevedo-Trejos et al., 2013; Goes et al., 2014, Brun et al., 2015). Understanding the drivers of biogeographical patterns of phytoplankton communities in the Labrador Sea will provide insights about the habitat complexity of this area, in addition to elucidating the phytoplankton responses to future changes. Plankton community structure from the Labrador Sea has previously been assessed by bio-optical, pigment or microscopic observations (Head et al., 2000; Stuart et al., 2000; Cota et al., 2003; Strutton et al., 2011; Harrison et al., 2013). Nonetheless, a detailed quantitative taxonomic analysis of the environmental controls on phytoplankton communities and species composition has not previously been carried out.

Based on *in situ* observations collected in the Labrador Sea during late spring and early summer (2011 – 2014), the specific goals of this study were:

1) to describe the biogeographical patterns of spring phytoplankton communities across the Labrador Sea,

2) to investigate the major hydrographic parameters that influence taxonomic segregation of phytoplankton blooms from the upper 50 m in the Labrador Sea,

3) to discuss the major environmental drivers for specific phytoplankton groups (e.g. *Phaeocystis pouchetii* and diatoms) in this high latitude sea.

2. Methods

2.1 Study area

The Labrador Sea and the entire subpolar North Atlantic receive buoyant fresh and cold Arctic outflow (Yashayaev et al., 2015) through two major pathways. One of these pathways connecting the Labrador Sea to the Arctic Ocean originates from the Baffin Island Current that crosses Davis Strait and subsequently merges with various southward inshore flows to become the Labrador Current (LC) (Fig. 1). The other pathway starts with the East Greenland Current (EGC) in the Greenland Sea (Yashayaev and Seidov, 2015), which turns around the southern tip of Greenland and flows northwards along the Greenland coast to become the West Greenland Current (WGC)(Yashayaev, 2007) (Fig. 1). The LC is composed of two main branches: an inshore branch, which occupies the Labrador Shelf, and an offshore branch, which is centred over the 1000 m contour. The inshore branch receives waters of Arctic origin via Davis and Hudson Straits, whereas the offshore branch receives contributions from the outflow from Davis Strait and from the portion of the WGC that turns west and then south along the shelf-break (Head et al., 2013) (Fig. 1). The inflow from Hudson Strait contains a large riverine input from Hudson Bay, increasing the contribution of estuarine waters to this water mass (15% of total volume of the LC) (Straneo and Saucier, 2008). Local ice melting also influences the properties of the LC, given that the Labrador Shelf is a seasonal ice zone, where sea ice starts forming in mid-January, reaching its maximum at the end of March and starts to melt in May (Wu et al., 2007).

147 The shallow fresh and cold WGC presents a mixture of low salinity Arctic water from
148 the EGC and Greenland ice melt (collectively sourced from glaciers, icebergs and Greenland
149 ice surface melts). The WGC is also influenced by the relatively warm and saline Atlantic
150 water, which, in turn, originates from the Irminger Current (IC) (Yashayaev, 2007, 2015)
151 (Fig. 1). Sea ice is prevented from forming on the Greenland Shelf, although icebergs are
152 frequent (De Sève, 1999; Yankovsky and Yashayaev, 2014). The deep central basin (water
153 depths from 3200 to 3700 m) of the Labrador Sea features a clockwise (anticyclonic)
154 circulation, which in turn contributes to an anticlockwise (cyclonic) gyre nested along the
155 outer rim of the deep basin (Yashayaev, 2007; Hall et al., 2013; Kieke and Yashayaev, 2015)
156 (Fig. 1).

157 The Labrador Sea is a region with complex, yet, well-structured hydrography
158 characterised by marked fronts maintained by the major currents such as the LC, IC and
159 WGC. These oceanographic fronts separate characteristic zones composed of distinct water
160 masses (Yashayaev, 2007). Boundary currents are concentrated at the Greenland and
161 Labrador slopes, where anticyclonic/cyclonic mesoscale eddies are common, particularly
162 Irminger Rings, located in the eastern part of the Labrador Sea (Frajka-Williams et al., 2009;
163 Yebra et al., 2009).

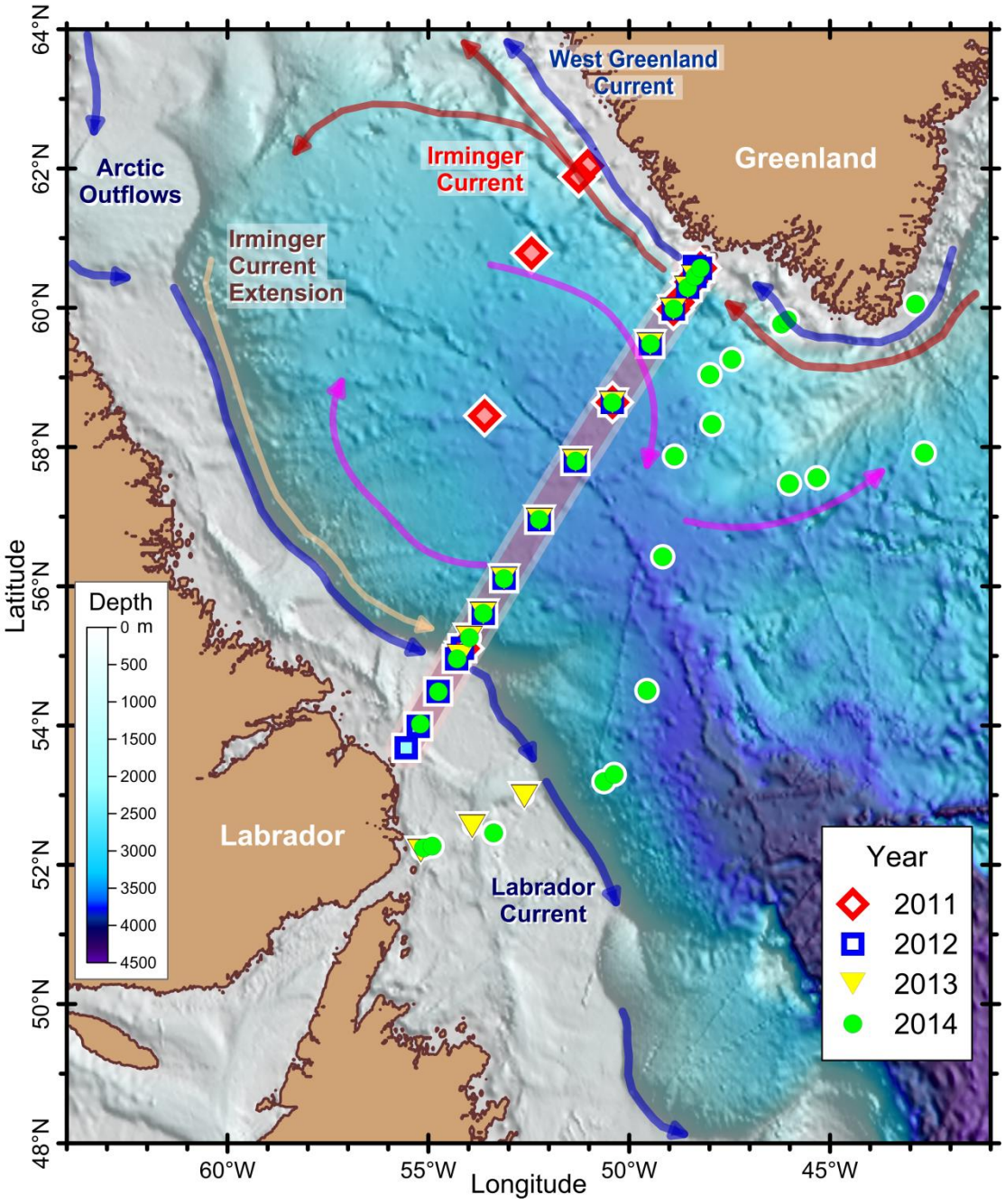

Figure 1. Map showing the stations and currents of the Labrador Sea. Stations were sampled along the AR7W transect (background line) during multiple years (2011 - 2014) or near the transect in 2011 (red diamonds), 2012 (blue squares), 2013 (inverted triangles), and 2014 (green dots). Scale refers to bathymetry. Circulation elements - colder currents (Labrador Current, Arctic Outflows and West Greenland Current, blue solid arrows), warmer currents (Irminger Current and Extension, red and brown solid arrows, respectively) and the anticyclonic circulation gyre (pink solid arrows) of the Labrador Sea.

2.2 Sampling

Initiated as a part of the *World Ocean Circulation Experiment* (WOCE), and then included as a key component into the *Climate and Ocean: Variability, Predictability and Change* (CLIVAR) sampling plan, the oceanographic section AR7W (following WOCE terminology) running across the Labrador Sea has been occupied annually by the *Ocean and Ecosystem Science Division* of the *Bedford Institute of Oceanography* (BIO) since 1990. This sustained full-depth sampling and monitoring of one of the most critical ocean basins includes collection and analysis of a broad variety of physical, chemical, and biological observations across the Labrador Sea and has recently been established as the principal component of the *Atlantic Zone Off-Shelf Monitoring Program* (AZOMP) of the *Department of Fisheries and Oceans Canada*. This section line, still commonly referred to as AR7W, extends from Misery Point just inshore of the Hamilton Bank on the Labrador Shelf to Cape Desolation on the Greenland Shelf (Fig. 1). The transect has 28 fixed position hydrographic stations when ice conditions do not prevent sampling on either of the shelves, in addition to some extra stations that are sampled, which vary annually.

Data for this study were collected on five research cruises (HUD-2011-009, HUD-2012-001, HUD-2013-008, HUD-2014-007, and JR302) to the Labrador Sea. The dates of the respective expeditions carried out by the *CCGS Hudson* (HUD-Year-ID) were May 11 - 17, 2011, 4 - 12 June, 2012, 9 - 21 May, 2013, and 7 - 14 May, 2014, and by the *RRS James Clark Ross* (JR302) – June 10 - 24, 2014. Stations were sampled on two transect crossings of the shelves and deep basin of the Labrador Sea (Fig. 1). The AR7W line was sampled annually on the *Hudson* with additional stations sampled south of the AR7W line in June 2014 on the JR302 cruise. In addition to these two transects, occasional other stations were also sampled in the Labrador Sea (Fig. 1).

Vertical continuous profiles of temperature, salinity and chlorophyll fluorescence were measured with a CTD/rosette system. Water samples were collected on the upward

CTD casts using 10-L Niskin bottles mounted on a rosette frame. Mixed layer depths were calculated from the vertical density (σ_Θ) distribution and defined as the depth where σ_Θ changes by 0.03 kg m^{-3} from a stable surface value (~10 m) (Weller and Plueddemann, 1996). As this mixed layer depth criterion presents limitations in accurately identifying weakly versus strongly stratified water masses, an additional and more robust criterion was used to measure stratification – a stratification index (SI). In this study, the SI was calculated as the difference in σ_Θ values between 60m and 10 m divided by the respective difference in depth (50 m).

For phytoplankton biomass determination from near surface waters of the Labrador Sea, mixed water samples from the upper 50 m (i.e. a mixture of 50 mL from each of 6 depths: 0, 10, 20, 30, 40, and 50m – (see Figure 9) and from the surface (<10 m) in case of samples from early summer 2014 (JR302 cruise) were collected and immediately preserved in acidic Lugol's solution to a final concentration of 2%. Samples were stored in dark glass bottles for later phytoplankton species identification and enumeration in the laboratory. Discrete water samples were collected for chlorophyll *a* (chl*a*) and nutrient analysis between the surface to a depth of 100 m at every 10 m or 25 m intervals (for more details, see Figure 9, supplemental material). Samples for nutrient analysis were frozen at -20°C and measured using an autoanalyzer (Alpkem RFA-300) or manually (ammonium, NH_4^+) using the hypochlorite method of Solórzano (1969) or the fluorometric method of Kerouel and Aminot (1997) (JR302 cruise). Chlorophyll *a* was extracted in 90% acetone for approximately 24 hours at -20°C and fluorometrically determined using a Turner Designs fluorometer (Holm-Hansen et al., 1965). Samples for particulate organic carbon (POC) were filtered (0.25 L – 1L) onto 25 mm pre-combusted GF/F filters and rinsed with 0.01 N HCl filtered seawater to remove inorganic carbonates and oven-dried (60ºC) for 8-12 hours. Samples were kept dry

and analysed in the laboratory using a Carbon-Hydrogen-Nitrogen (CHN) analyser (Collos, 2002).

2.3 Phytoplankton enumeration

Lugols preserved samples were counted to determine phytoplankton (> 4 μm) abundance and taxonomic composition. According to cell abundance (previously observed under the light microscope), 10 or 25-ml of each sample was placed in settling chambers for 24 h and examined using a Leiss inverted microscope under x100 or x200 magnification (Utermöhl, 1958). Large (> 50 μm) and numerically rare taxa were counted during full examination of the settling chamber at x100 magnification, while small (< 50 μm) and numerically dominant taxa were counted on 1 or 2 transects of the chamber at x200 magnification. At some stations where large taxa were dominant, such as the diatoms *Ephemera planamembranaceae* and *Thalassiosira* spp., at least 300 individuals were counted in 1 or 2 transects at x100 magnification. Counting units were considered as individuals cells, regardless of whether they were solitary or in a chain/colony, except for *Phaeocystis pouchetii* colonies, which were considered individuals categorized by colony size (small: <100 μm, medium: 100 - 199 μm, large: 200 - 299 μm and extra large > 300 μm). Cell abundance within each size category of colony was estimated as the average number of cells counted in at least 10 different colonies of that size category. *P. pouchetii* single cells, either - flagellated or derived from colonies, were counted and grouped together.

Diatoms and dinoflagellates were identified to genus or species whenever possible following Medlin and Priddle (1990), Tomas (1997) and Throndsen et al. (2007). Unidentified dinoflagellate taxa were grouped as small (4 - 29 μm) or large (>30 μm), and

with reference to cell wall structure (naked or armored). Unidentified diatoms were grouped as centric or pennate according to a size category (i.e. 4 - 19 μm, 20 - 49 μm, 50 - 99 μm, 100 - 149 μm, 150 - 200 μm and >200 μm). *Thalassiosira* and *Fragilariopsis* species identification were only possible using a Scanning Electron Microscope (SEM), except for *Fragilariopsis atlantica*, and therefore *Fragilariopsis* genus were also categorized by size: small (4 - 19 μm), medium (20 - 50 μm) and large (>50 μm). The genus *Chaetoceros* was also classified by size as large (subgenus *Phaeoceros*), medium (*C. decipiens*, *C. mitra*, *C. laciniosus*, *C. debilis*, *C. curvisetus*) or small (*C. compressum*, *C. socialis* and others which could not be identified to species level using the light microscope). It was not possible to identify most of the nanoflagellates, other than cryptophytes, *P. pouchetii* and small dinoflagellates, and therefore unidentified flagellates are not included in this study (median and standard error biomass = 12 ± 3% of total biomass).

2.4 Biovolume and biomass estimation

Cell biovolume was calculated based on geometrical shapes assigned for each taxa as suggested by Sun and Liu (2003). Cell dimensions of at least 10 specimens were measured and biovolume for each taxon was compared to the literature (Olenina et al., 2006). Cell carbon concentrations were estimated using carbon conversion factors for diatoms (Montagnes and Franklin, 2001) and other protists (Menden-Deuer and Lessard, 2000). For *P. pouchetii*, total carbon biomass consisted of cell biomass (either -flagellated, non-motile or colony-bound cells) and biomass contained in the mucus of *Phaeocystis* colonies. *P. pouchetii* cell carbon biomass was estimated based on geometrical shape as previously described, without any distinction between flagellate, non-motile or colony-bound cells. A mucus carbon conversion factor has previously been developed to convert from colony

volume to total colony biomass for *P. antarctica* (213 ng C mm^{-3}, Mathot et al., 2000) and *P. globosa* (335 ng C mm^{-3}, Rousseau et al., 1990). Given the lack of data on carbon estimates of colonial mucus for *P. pouchetii*, the average colonial mucus reported from *P. antarctica* and *P. globosa* was applied for *P. pouchetii* colonies in this study (i.e. 274 ng C mm^{-3}). A regression analysis ($y = 1.01x + 240.92$; $r^2 = 0.47$; $n = 44$; $p < 0.0001$) of the carbon calculated from cell counts and carbon derived from POC analysis showed good agreement. The goodness-of-fit was confirmed by visually observing the normal distribution of the residuals.

2.5 Statistical analyses

Phytoplankton community structure in the Labrador Sea during late spring and early summer of 2011 - 14 was investigated using PRIMER-E (v7) software (Clarke and Warwick, 2001). Biomass data from the 75 phytoplankton taxa (including species, genus and different morphotypes) were normalized by performing a square root transformation, allowing each taxon to influence the similarity within and among samples. Bray-Curtis similarity was calculated within each pair of samples and a Cluster analysis of this matrix was generated to display the similarity relationship among samples. An arbitrary threshold (46% of similarity) was applied to link the samples that are more similar to each other (i.e. > 46% similar in terms of taxa composition) into Cluster groups.

A non-metric multi-dimensional scaling (nMDS) plot was used to visually display the similarity relationship between the respective pairs of samples derived from Bray-Curtis similarity matrix. Thus, samples that reflected greater community resemblances were spatially closer than the ones that were less similar. The stress level of the nMDS plot is a measurement of how accurate the representation is, with lower stress values being associated

with better visual representation of the similarity relationship in 2-D space. Bubble plots were constructed in the nMDS plots to identify the associations between blooms (in terms of carbon biomass and chl*a*) and physical parameters (MLD and SI). For this analysis, a threshold of median chlorophyll *a* biomass values greater than 1.2 mg chl*a* m^{-3} for each Cluster was applied to arbitrarily define bloom conditions at the upper 50 m.

The similarity percentage analysis (SIMPER) routine was used to explore the dissimilarities between Clusters and the similarities within Clusters of samples. Moreover, this output was used to identify the contributions from each taxon to the (average) overall similarity within Clusters at a cutoff of 90% cumulative contribution. A post-hoc analysis of similarity (one-way ANOSIM) was also applied to determine whether Clusters were statistically significantly different from each other in terms of their taxonomic composition.

To analyse the effects of gradients (environmental parameters) on the Labrador Sea phytoplankton biomass and community structure, a redundancy analysis (RDA) was performed using the CANOCO 4.5 software (CANOCO, Microcomputer Power, Ithaca, NY). This multivariate analysis determines the environmental variables (explanatory variables) that best explain the distribution of the major selected taxa, by selecting the linear combination of environmental variables that yields the smallest total residual sum of squares in the taxonomic data (Peterson et al., 2007). Only taxa that contributed to more than 0.5% of total biomass (reduced from 75 to 11 taxa) were selected for RDA analysis. Detrending canonical correspondence analysis (DCCA) was used *a priori* to determine whether the data ordination method was linear (suitable for RDA analysis) or unimodal (suitable for Canonical Correspondence Analysis – CCA). A relatively small gradient length (< 2.5 standard deviation units according to DCCA analysis output) revealed that the ordination was linear-based and that RDA analysis was suitable (Lepš and Šmilauer, 2003). Forward-selection (*a posteriori* analysis) was used to identify a subset of environmental variables that significantly

explained taxonomic distribution and community structure when analysed individually (λ_1, marginal effects) or included in the model where other forward-selected variables were analysed together (λa, conditional effects). Biomass data were log-transformed and a Monte Carlo permutation test (n = 999, reduced model) was applied to test the statistical significance ($p < 0.05$) of each of the forward-selected variables.

3. Results

3.1 Hydrography and nutrient distributions

The Labrador Sea was divided into five distinct zones based on its bathymetry – a wide and shallow shelf (< 250 m) and slope (250 m – 1000 m) located close to Canada (Labrador Margin), a deep central Basin (> 2500 m) and a narrow and steep slope (2500 m – 3000 m) and shelf (< 2500 m) on the Greenland Margin (Fig. 2a). Temperature and salinity from surface and sub-surface waters (upper 50 m) varied among these distinct zones across the Labrador Sea (Fig. 2b). In general, colder (temperature < 2°C), fresher (salinity < 34) and less dense waters (σ_θ < 27 kg m^{-3}) were found on the shelves and slope regions (Fig. 2b), particularly on the Labrador Shelf and Slope and at the Greenland Shelf during late June (see the arrows in Fig. 2a and b), indicating the influence from the Arctic outflow. A warmer (temperature > 1°C), saltier (salinity > 33.5) and denser (σ_θ > 27 kg.m^{-3}) water mass with features of modified Atlantic waters (Irminger Current, IC) was found widely distributed in the central portion and Greenland slope of the Labrador Sea (Fig. 2). The temperature and salinity (T-S) properties from the surface and subsurface waters varied interanually (2011 - 2014) and seasonally (from early May until late June) during the period of study (Fig. 2b).

In spite of the interannual variability, the T-S properties of the surface/subsurface waters of most stations on the Labrador Shelf were generally colder and fresher (average T =

-0.6°C and salinity = 32.6) than the waters on the Greenland Shelf (average T = 0.3°C and salinity = 33.1) during May, suggesting that the former was influenced by direct inputs of fresher and colder water from the Arctic, Hudson Bay, continental run-off and from local sea-ice melt (Fig. 2b). However, instances of extremely fresh and cold waters were also found in late June 2014 at some stations south of Greenland, suggesting the influence of additional glacial melt in this region (Fig. 2b, see arrows). The positions of fronts, usually recognised by a sharp gradient between Arctic and modified Atlantic (Subpolar Mode and IC) waters, varied from year to year, but were generally located near the continental slopes (data not shown).

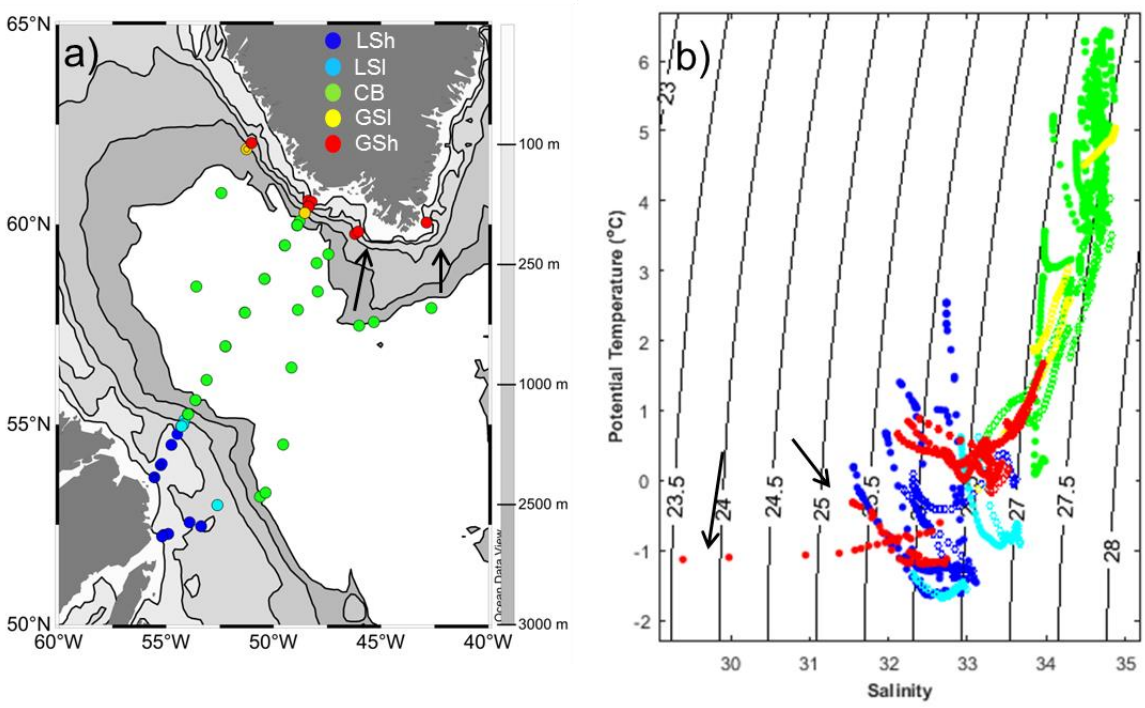

Figure 2. Biogeographical zones in the Labrador Sea classified by bathymetry: (a) Labrador Shelf (LSh), Labrador Slope (LSl), Central Basin (CB), Greenland Shelf (GSh) and Greenland Slope (GSl); and (b) potential temperature and salinity (T-S) with isopycnals (σ_θ) scatter plot of the upper 50 m waters from these five zones during May (open circles) and June (closed circles) of 2011 -2014. Arrows indicate the stations on the Greenland Shelf and the corresponding T-S signature during late June 2014.

Nutrient concentrations from the surface and subsurface waters (upper 50 m) varied spatially and temporally across the Labrador Sea (Fig. 3). In general, the temporal variation

in nutrient concentrations (nitrate, silicate, phosphate and Si* (silicate minus nitrate concentration)) had similar trends during May and June (Fig. 3a-f, 3i-l), except ammonium concentrations, which were clearly higher in the Central Basin and Greenland Shelf and Slope (median > 0.8 µM) during June (Fig. 3g,h). In general, nitrate, silicate and phosphate concentrations were lowest on the Greenland Shelf and Slope (Fig. 3a-f). Median nitrate concentrations were clearly higher in the Central Basin (> 8 µM in May and > 5 µM in June), (Fig. 3c,d). Median silicate concentrations were greater in the central western part of the Labrador Sea (Labrador Shelf and Slope, and Central Basin), where median concentrations were > 5 µM in May and > 4 µM in June (Fig. 3a,b). Phosphate concentration was higher in the western part of the Labrador Sea, on the Labrador Shelf and Slope (median > 0.8 µM in May and > 0.5 µM in June) and decreased eastwards (Fig. 3e,f).

The central Basin had median Si* < 0 µM, which suggests that the phytoplankton from these regions experienced, in most cases, an excess of nitrate compared to silicate (median Si* = -4 µM during May and -1 µM during June, respectively), although there were some stations in the central Basin region where Si* values were > 0 µM (Si* up to 4 µM) (Fig. 3i,j). The Labrador Shelf had higher median Si*, particularly during June (Si* up to 1 µM) (Fig. 3j) and the Greenland Shelf had Si* values approaching zero (Fig. 3i,j). The Labrador Shelf also had higher Si* values at depth (Si* from -6 µM up to -1 µM approximately at 200 m or the deepest depth if bottom depth is < 200 m) compared to the other regions (Si* < -4 µM), although in general, these waters had an excess of nitrate compared to silicate (i.e. negative values, Fig. 3k,l). Higher Si* in shelf waters, particularly on the Labrador Shelf, may be associated with input of riverine and glacial meltwaters enriched with silica.

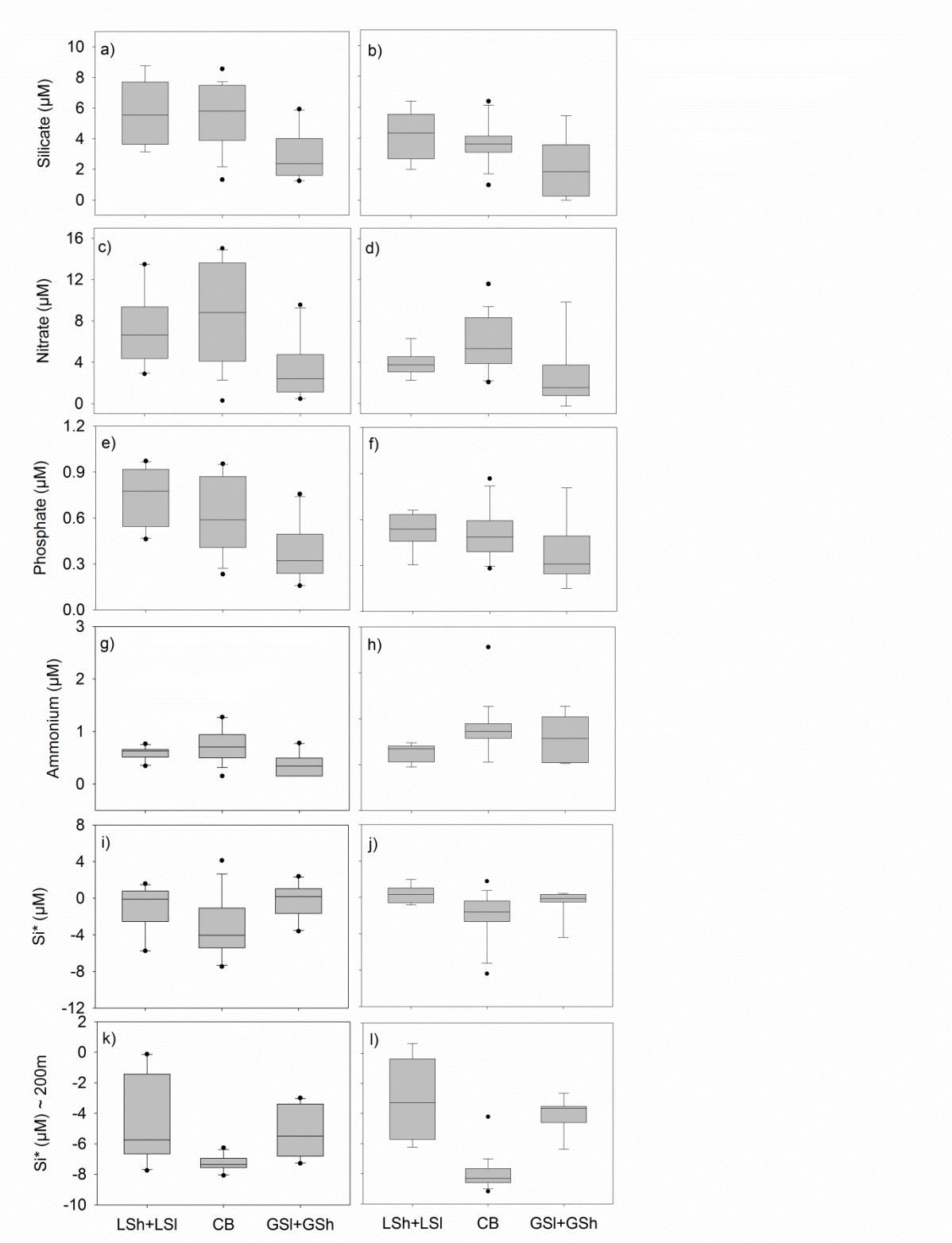

Figure 3. Boxplots (median, upper and lower quartile, minimum and maximum values and outliers) of (a,b) silicate, (c,d) nitrate, (e,f) phosphate and (g,h) ammonium concentrations, in addition to (i,j) Si* (silicate minus nitrate concentrations) from the upper 50 m and (k,l) from approximately 200 m water depth in May (left) and June (right) among each biogeographical zone of the Labrador Sea: Labrador Shelf (LSh) + Labrador Slope (LSl), Central Basin (CB) and Greenland Slope (GSl) + Greenland Shelf (GSh).

396

397 *3.2 Chlorophyll a concentrations*

398 Chlorophyll *a* biomass was concentrated within subsurface waters (upper 50 m) of the
399 Labrador Sea (Figure 8 and 9, supplemental material). Thus, average concentrations of
400 chlorophyll (upper 50 m) were used to show the spatial variation of subsurface blooms across
401 the Labrador Sea. The chlorophyll *a* distribution (average of the upper 50 m) varied spatially
402 and interannually (Fig. 4). In general, the eastern Labrador Sea, near and within the
403 Greenland Slope and Shelf waters, had the highest subsurface (< 50 m) concentrations of
404 chlorophyll *a*, particularly during May 2011 and 2013 (Fig. 4a,c; average >10 mg chl*a* m^{-3}).
405 The Labrador Shelf and Slope also had relatively high near surface chlorophyll *a* values (>5
406 mg chl*a* m^{-3}) in all years, except during May 2014, possibly because sampling was before the
407 formation of the bloom (Fig. 4d). The offshore waters of the central Basin generally had
408 lower near surface chlorophyll *a* concentrations (<5 mg chl*a* m^{-3}) than the shelves in May,
409 but later in the season (June 2012, 2014) average subsurface chlorophyll *a* values were ~ 5
410 mg chl*a* m^{-3} (Fig. 4b,e).

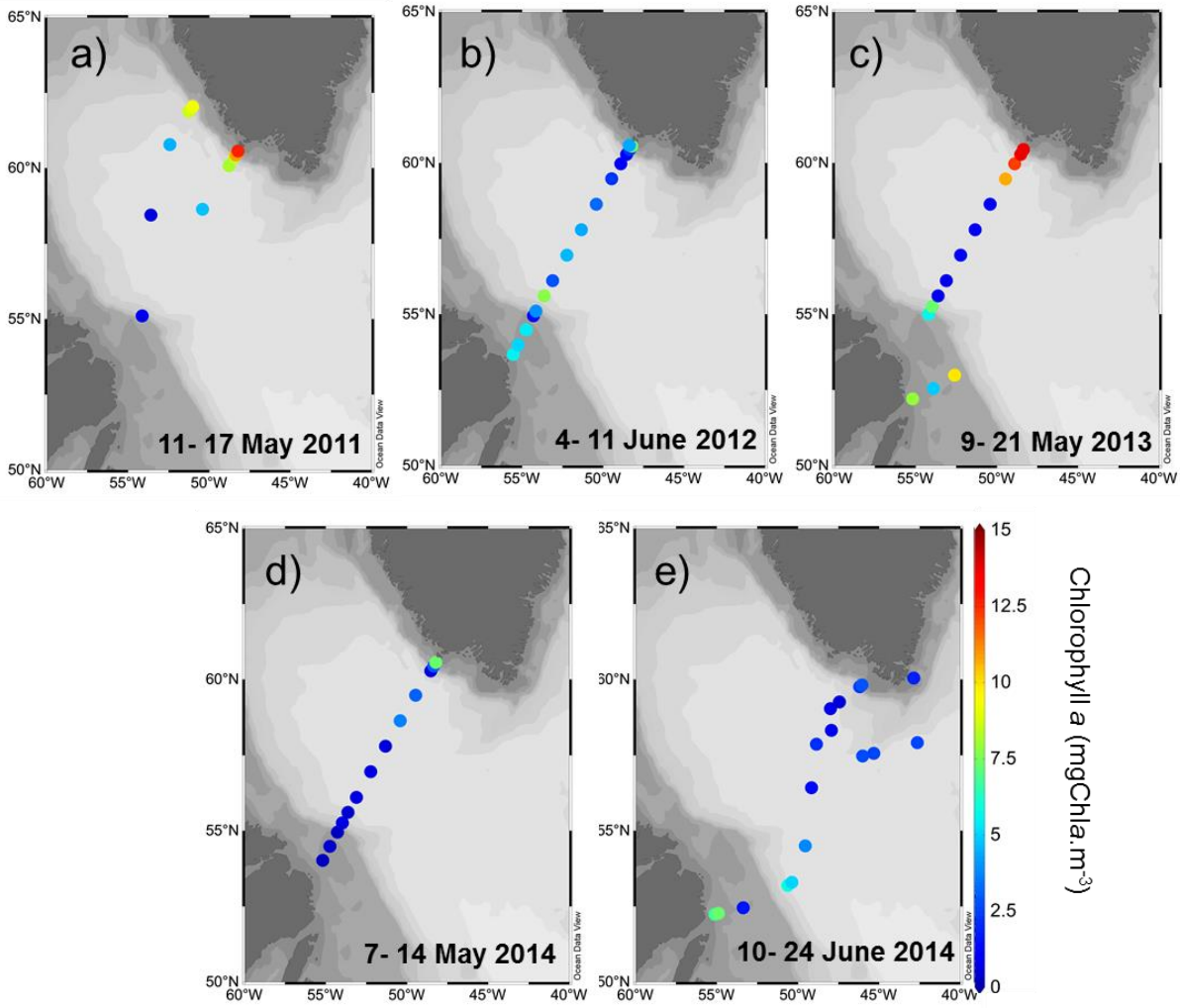

411

412 Figure 4. Chlorophyll *a* distribution (average of 0 – 50 m values) at each station of the Labrador Sea
413 during late spring/early summer 2011 - 2014 (a-e). Cruise dates are given in each panel.

414

415 *3.3 Phytoplankton community structure*

416 Cluster analysis of phytoplankton biomass from the Labrador Sea during spring and
417 summer of 2011 - 2014 distinguished seven major Clusters of samples with a similarity level
418 of 46%. Non-metric multi-dimensional scaling (nMDS) analysis showed a two-dimensional
419 spatial representation of the similarities within sampled stations based on the composition and
420 biomass values (Fig. 5a). A stress level < 0.2 in the nMDS plot (Fig. 5a) corresponds to a
421 'suitable' two-dimensional representation of the similarity relationships of the samples within
422 and between Clusters (as defined in Clarke, 1993). ANOSIM one-way analysis comparing

each Cluster suggested that they were significantly different in composition ($p = 0.001$, R statistic from pairwise analysis varied from 0.75 – 1), and that the Cluster groups are well separated, given that the R statistic values are approaching 1 (see Clarke and Warwick, 2001). Taxa whose cumulative contribution approximated 90% of the average similarity within each Cluster are shown in Table 1.

Cluster 1 (n = 12) included the samples from the Labrador Shelf during June 2012 and 2014 and May of 2013 (Fig. 5c, d, f). This Cluster had the second highest average biomass (275 ± 131 mg C m^{-3}) compared to the other Clusters identified, with large contributions to the Group similarity from Arctic and sea-ice diatoms, such as *Thalassiosira* spp. (particularly *T. hyalina*), *Porosira glacialis*, *Fragilariopsis* spp. (particularly *F. cylindrus* and *F. oceanica*), *Fossula arctica*, *Bacterosira bathyomphala*, *Chaetoceros* spp. (e.g. *C. socialis* and *Phaeoceros*) (Table 1) and *Coscinodiscus centralis*, in addition to unidentified small dinoflagellates (< 30 μm), *Gyrodinium* spp., *Protoperidinium* and cryptophytes (Table 1).

Cluster 2 (n = 10) contained samples with relatively high biomass (average of 169 ± 105 mg C m^{-3}) compared with Clusters 3, 6 and 7 but lower than Clusters 1, 4 and 5. These samples were from offshore waters of the centre of the Labrador Sea during June (early summer - 2012, 2014) (Fig. 5c,f). Sub-arctic North Atlantic diatoms, such as *Ephemera planamembranacea*, and *Fragilariopsis atlantica*, in addition to *Thalassiosira* spp. and dinoflagellates (unidentified small and large armored, *Gyrodinium* spp.) all contributed to the similarity of these samples (Table 1).

Dinoflagellates (unidentified small and *Gyrodinium* sp.), cryptophytes, silicoflagellates (*Dictyocha speculum*) and the diatom *Pseudo-nitzschia* spp. contributed to the similarity of samples in Cluster 3 (n = 12) (Table 1). These samples had the lowest

446 average biomass overall (5 ± 4 mg C m^{-3}) and came from the western-central region of the
447 Labrador Sea during May 2011, 2013, 2014 (late spring) (Table 1, Fig. 5b,d,e).

448 Cluster 4 (n = 8) included samples with the highest biomass overall (average = 304 ±
449 282 mg C m^{-3}) where the diatom *Rhizosolenia hebetata f. semispina* was the major
450 contributor to the similarity between samples (64%) (Table 1). Other diatoms, including
451 medium to large *Chaetoceros* spp. (e.g. *C. decipiens* and *Phaeoceros*) and *Pseudo-nitzschia*
452 *granii*, dinoflagellates (unidentified naked), cryptophytes and the prymnesiophyte
453 *Phaeocystis pouchetii* contributed up to almost 90% of the cumulative similarity (Table 1).
454 Samples from this Cluster occurred only in the central region of the Labrador Sea and later in
455 the season (mid-summer; late June) during 2014 (Fig. 5f).

456 The prymnesiophyte *Phaeocystis pouchetii* was the major contributor to samples in
457 Cluster 5 (n = 28), with the third highest average biomass (248 ± 181 mg C m^{-3}) (Table 1).
458 Diatoms such as *Thalassiosira* spp., *Rhizosolenia hebetata f. semispina*, *Pseudo-nitzschia*
459 *granii*, *Porosira glacialis* and *Chaetoceros* (*Phaeoceros*, but mostly *C. socialis*), in addition
460 to dinoflagellates (small unidentified and *Gyrodinium* spp.) also contributed cumulatively to
461 almost 90% of similarity of these samples (Table 1). Samples from Cluster 5 also had the
462 highest average chlorophyll *a* biomass (Table 2) and occurred in the central-eastern section of
463 the Labrador Sea (along and/or on the nearby Greenland shelf) during all years (2011 - 2014)
464 (Fig. 5b-f).

465 Cluster 6 (n = 2) comprised two samples from Greenland Shelf waters during summer
466 2014 (Fig. 5f), with relatively low biomass (87 ± 14 mg C m^{-3}) (Table 1). Small (e.g. *C.*
467 *socialis*) and medium-sized diatoms, such as *Chaetoceros* spp. (e.g. *C. decipiens*),
468 *Thalassiosira* spp. and *Rhizosolenia hebetata f. semispina*, in addition to the flagellate *P.*
469 *pouchetii* contributed up to 77% of the similarity for these samples (Table 1).

Cluster 7 (n = 2) stations also had relatively low average biomass (33 ± 4 mg C m^{-3}) and was comprised of just two samples from the central Labrador Sea during May 2013 (Table 1, Fig. 5d). Samples from this Cluster represent a mixture of Clusters 3 and 5, where diatoms such as *Pseudo-nitzschia* spp., *Thalassiosira*, *Rhizosolenia hebetata f. semispina*, *Corethron criophilum*, in addition to *P. pouchetii* and dinoflagellates (small unidentified naked) contributed mostly to the similarity for these samples (Table 1).

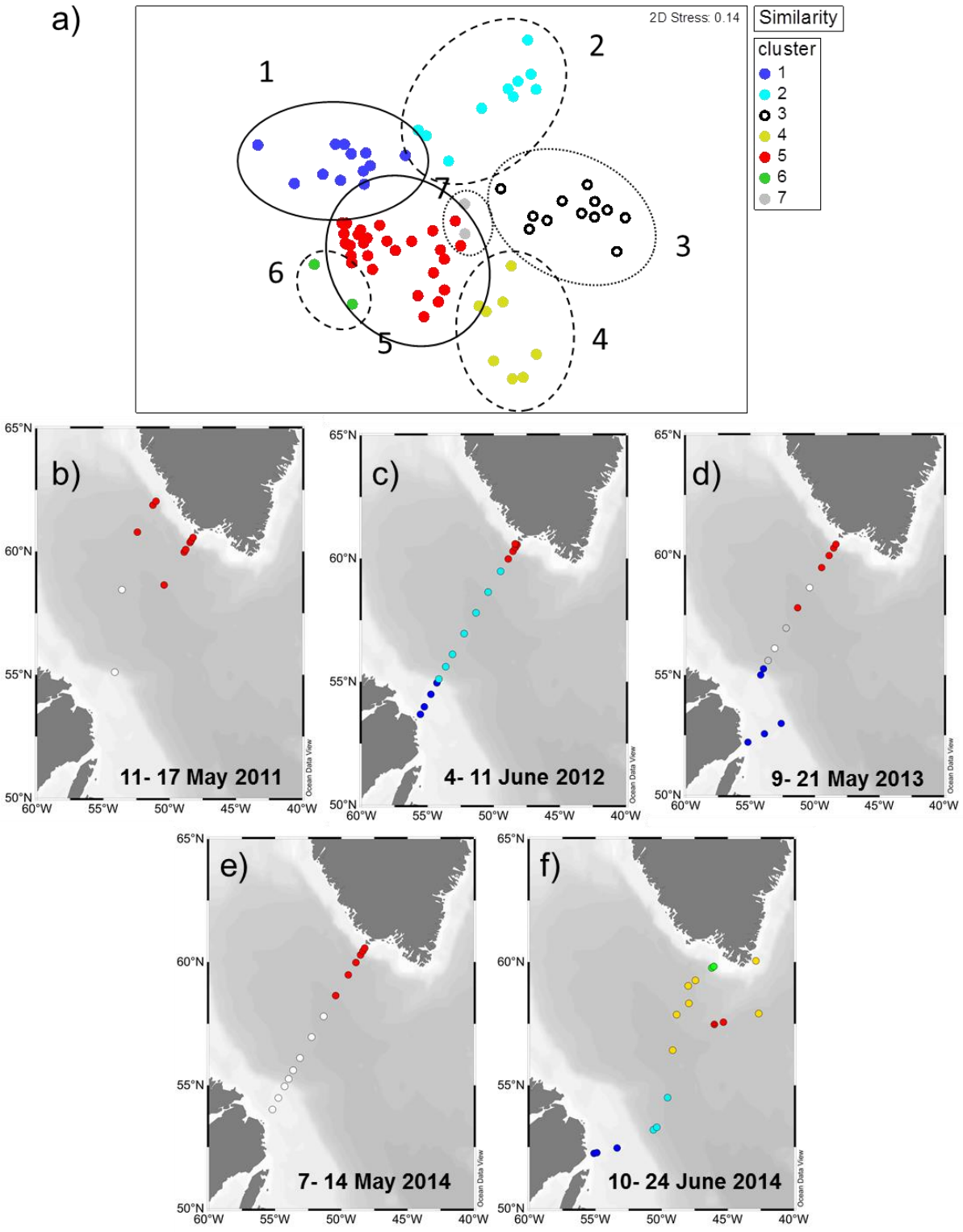

Figure 5. Cluster analysis of phytoplankton community composition across the Labrador Sea and multiple years. (a) Non-metric Multi-dimensional scaling (nMDS) plot representing the similarity in phytoplankton community structure within sampled stations at 46% similarity level (outlines) based on carbon biomass values. Temporal aspects of the Clusters from communities observed during May and June (solid outline), May only (dotted outline) or June only (dashed outline) are revealed on the outlines that separates each Cluster. (b - f) Distribution maps of distinct Clusters represented in the nMDS plot at each station of the Labrador Sea during May and June of 2011 - 2014.

Table 1. Percentage contribution of each taxa to the similarity of sampled stations, cumulative contribution up to approximately 90% and average similarity and biomass within each cluster. Numbers in bold refer to taxa whose cumulative contribution were up to approximately 70%. See methods for size (small, medium, large) classification. NI.- non-identified genus/species.

Taxa	Cluster 1	Cluster 2	Cluster 3	Cluster 4	Cluster 5	Cluster 6	Cluster 7
Armored dinoflagellates NI	2.6	**5.8**	**13.1**				2.8
Bacterosira bathyomphala	2.4						
Chaetoceros spp. (medium)				1.9		**11.5**	
Chaetoceros spp. (small)	1.4				2.7	**30.6**	
Corethron criophilum							**7.4**
Coscinodiscus centralis	1.1						
Cryptophytes	1.5		**22.8**	2.9			**5.5**
Dictyocha speculum			1.9				
Ephemera planamembranaceae		**49.5**					2.1
Eucampia groelandica							**3.8**
Fossula arctica	**3.7**						
Fragilariopsis atlantica		4.8					
Fragilariopsis spp. (large)	**3.6**						2.2
Fragilariopsis spp. (medium)	**6.1**					3.4	2.9
Fragilariopsis spp. (small)	3						1.6
Gyrodinium spp.	2.1	4.9	7		1.9	2.9	
Naked dinoflagellate NI (large)		3.6	4.5				2.3
Naked dinoflagellates NI (small)	**5.2**	**12**	**32**	**8.7**	4.9		**10**
Nitzschia spp.							1.6
Phaeoceros spp.	1.9			6.8	2.2		2.3
Phaeocystis pouchetii				4.7	**42**	6.9	**6.5**
Porosira glacialis	**24.1**				3	2.8	
Protoperidinium spp.	1.7	**7.5**				5.4	
Pseudonitzschia granii				2.6	3.3		2.5
Pseudo-nitzschia spp			1.9				**14.3**
Rhisozolenia hebetata f.				**64.2**	3.3	**9**	**10.1**
Thalassiosira spp.	**30.1**	5.2	**8.4**		**27.1**	**19.2**	**13.9**
Cumulative contribution (%)	90.3	93.4	91.5	91.7	90.3	91.7	91.6
Average similarity	59.7	60.1	56.2	62.8	57.1	74.4	79.7
Average biomass (mgC.m^{-3})	275±13	169±10	5±4	304±28	248±18	87±14	33±4

3.4 Hydrographic influence on phytoplankton community structure

Hydrographic variables that explained the variance (explanatory variables) in the biomass of selected phytoplankton taxa (biomass greater than 0.5% of total) were investigated using redundancy analysis (RDA). The ordination diagram (Fig. 6) revealed associations between each taxon and the explanatory variables. Proximity of taxa to the environmental variables (arrows) in the same or opposite direction suggests positive or negative correlations, whereas no proximity indicates weak or a lack of correlation; the

longer the arrow, the stronger the correlation. The associations in the ordination diagram show that Arctic diatoms (Cluster 1, such as *Fossula arctica, Coscinodiscus, Fragilariopsis* spp., *Porosira glacialis* and *Thalassiosira* spp., in addition to *Chaetoceros* spp., particularly *C. socialis* - Cluster 6) occurred in colder (median temperature < 0°C), fresher (median salinity < 33.0) and more stratified waters (median SI > 14 x 10^3 kg m^{-4}) (Table 2).

Phaeocystis pouchetii (Cluster 5) dominated in waters where nutrient concentrations (mainly nitrate, but also phosphate and silicate) were low (median nitrate concentration < 3.7 μM) (Table 2). *Ephemera planamembranaceae* (Cluster 2) and *Rhizosolenia hebetata f. semispina* (Cluster 4) were found in relatively warmer waters (median > 4.7°C) with higher salinities (median > 34.5). Dinoflagellates (unindentified small and *Protoperidinium*, Clusters 3 and 7) were common in less stratified waters (median SI = 0.1 x 10^3 kg m^{-4}) and higher nitrate (median > 9 μM), phosphate (median > 0.7 μM) and silicate (median > 4.5 μM) concentrations (i.e. pre-bloom conditions) (Fig. 6, Table 2).

The first axis (x- axis) of the analysis explained most of the variance (eigen-value = 23.9%, cumulative percentage variance between taxa and environmental factors = 58.0%), whereas all canonical axes explained 98.3% of the variance (axis 1, p = 0.001; all axes, p = 0.001) (Fig. 6, Table 3). This means that (1) the arrows displayed closer to the x-axis explained most of the variability in the data, and that (2) environmental variables explained almost 100% of the variation of the selected taxa, when all four axes were analysed together.

Forward selection showed that of all seven environmental factors (Table 3) included in the analysis, only four (temperature, nitrate, salinity and phosphate) best explained the variance in the phytoplankton taxa biomass when analysed together. When all the forward-selected variables were analysed together (conditional effects, referred to as λ_a in Table 3), temperature was the most significant explanatory variable (λ_a = 0.16, p = 0.001), followed by

nitrate concentration and salinity (λ_a = 0.1, p = 0.001) (Table 3). Phosphate concentration was also a significant explanatory variable (λ_a = 0.03, p = 0.048) (Table 3). Although not significantly (p < 0.05) different (λ_a = 0.01, p = 0.094), silicate concentrations also had a slight influence as an explanatory variable (Table 3). Ammonium concentration and SI were not significant explanatory variables in this study.

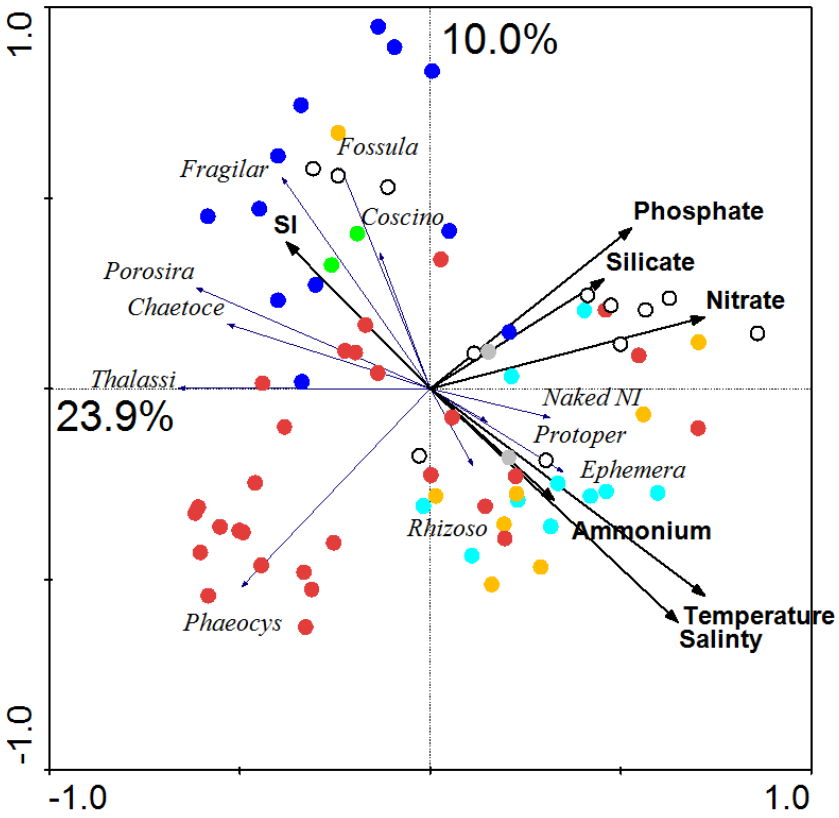

Figure 6. Ordination diagram generated from redundancy analysis (RDA). Triplot represents taxa carbon biomass (thin lines), the significant explanatory variables (thick lines) and samples/stations (closed circles; colours refers to cluster groups on Figure 5a). Chaetoce = small *Chaetoceros* (mostly *C. socialis*), Coscino= *Coscinodiscus centralis*, Ephemera = *Ephemera planamembranaceae*, Fossula = *Fossula arctica*, Fragilar = *Fragilariopsis* medium (mostly *F. cylindrus*), Naked NI = Small (< 30 µm) naked unidentified dinoflagellates, Phaeocys = *Phaeocystis pouchetii*, Porosira = *Porosira. glacialis*, Protoper = *Protoperidinium* spp., Rhizoso = *Rhizosolenia* spp., Thalassi = *Thalassiosira* spp. SI= Stratification Index.

Table 2. Median and standard error of hydrographic and biological parameters of each cluster. MLD= Mixed layer depth, SI= Stratification index.

Parameters	Cluster 1	Cluster 2	Cluster 3	Cluster 4	Cluster 5	Cluster 6	Cluster 7
σθ (kg.m^{-3})	26.2 ± 0.1	27.3 ± 0	27.6 ± 0.2	27.4± 0.2	27.1 ± 0.1	25.8 ± 0	27.5 ± 0.1
Salinity	32.6 ± 0.1	34.6 ± 0.1	34.8 ± 0.2	34.6 ± 0.4	33.9 ± 0.1	32.1 ± 0.1	34.6 ± 0.1
Temperature (°C)	-0.3 ± 0.2	4.8 ± 0.4	3.3 ± 0.6	4.9 ± 0.8	1.6 ± 0.3	-0.7 ± 0	3.3 ± 0
Silicate (µM)	4.3 ± 0.4	3.7 ± 0.3	7.6 ± 0.5	2.8 ± 0.6	3.5 ± 0.3	0.3 ± 0.1	4.7 ± 0.8
Phosphate (µM)	0.6 ± 0	0.5 ± 0.1	0.9 ± 0	0.4 ± 0.1	0.4 ± 0	0.2 ± 0	0.8 ± 0.1
Nitrate (µM)	3.8 ± 0.3	5.4 ± 0.7	13.4 ± 0.9	4.5 ± 1.2	3.6 ± 0.6	0.8 ± 0	9.9 ± 1.0
Si*	0.3 ± 0.1	-2.0 ± -0.6	-5.6 ± -1.6	-0.8 ± -0.3	-0.4 ± -0.1	-0.4 ± -0.3	-5.2 ± -3.7
Ammonia (µM)	0.4 ± 0.1	0.7 ± 0.1	0.5 ± 0.1	0.6 ± 0.3	0.6 ± 0.1	0	1.1 ± 0.1
MLD (m)	19.5 ± 1.4	20.0 ± 3.3	76.0 ± 89.5	24.0 ± 2.3	24.5 ± 4.9	15.0 ± 0	87.5 ± 3.5
C biomass (mgC.m^{-3})	262 ± 38	147 ± 33	4.0 ± 1.0	251 ± 100	228 ± 34	87 ± 10	33 ± 3
Chlorophyll (mgchl*a*.m^{-3})	5.6 ± 0.7	4.0 ± 0.5	0.5 ± 0.1	1.4 ± 0.2	5.9 ± 0.8	2.5 ± 0.3	1.0 ± 0.2
Stratification Index	14.9 ± 4.8	6.6 ± 0.6	0.1 ± 0.4	7.4 ± 2.2	5.1 ± 1.2	16.0 ± 2.3	0.1 ± 0.01

Table 3. Variance explained by each explanatory variable (temperature (°C), nitrate, phosphate, silicate and ammonium (μM), salinity and SI (kg m^{-4})) when analysed alone (λ_1, marginal effects) or when included in the model where other forward-selected variables are analysed together (λa, conditional effects). Significant *p-values* (**p< 0.05) and (*p<0.1) represents the variables that, together, significantly explain the variation in the analysis. SI= Stratification Index.

Marginal Effects					Conditional Effects			
Variable	λ_1				Variable	λ_a	*P*	*F*
Temperature	0.16				Temperature	0.16	0.001*	13.37
Nitrate	0.15				Nitrate	0.1	0.001*	9.72
Salinity	0.14				Salinity	0.1	0.001*	10.77
Phosphate	0.11				Silicate	0.01	0.094*	1.88
Silicate	0.09				Phosphate	0.03	0.043*	2.44
SI	0.07				Ammonium	0.01	0.283	1.2
Ammonium	0.04				SI	0	0.665	0.62
Axes	1	2	3	4	Total variance			
Eigen-values	0.239	0.100	0.056	0.010	1			
Taxa-environment correlations	0.760	0.727	0.809	0.540				
Cumulative percentage variance								
of species data	23.9%	33.9%	39.5%	40.5%				
of species-environment relation	58.0%	82.3%	95.9%	98.3%				
Sum of all eigen-values					1			
Sum of all canonical eigen-values					0.412			

Test of significance of first canonical axis: eigen-value = 0.239; F-ratio = 20.702; P-value = 0.001 **
Test of significance of all canonical axis: Trace = 0.412; F-ratio = 6.606; P-value = 0.001**

3.5 Bloom development

To investigate the influence of hydrography on near surface (< 50 m) bloom development, MLD and SI were compared with Clusters that had a large biomass in terms of carbon and chlorophyll *a*. Five blooms (average chlorophyll *a* > 1.2 mg chl*a* m^{-3} per Cluster, see methods) belonged to Clusters 1, 2, 4, 5 and 6 and were composed of distinct phytoplankton communities observed in this study (Table 1). Shelf blooms, such as those located near or within Greenland Shelf waters (Clusters 5 and 6) and on the Labrador Shelf

(Cluster 1) had the highest biomass values, particularly Clusters 5 and 1 (median chl*a* = 5.9 ± 0.8 mg chl*a* m^{-3} and 5.6 ± 0.7 mg chl*a* m^{-3}, respectively) (Table 2, Fig. 7a,b). Central Basin blooms (Clusters 2 and 4) were weaker than shelf blooms (average values of chlorophyll *a* concentration were 4.0 ± 0.5 mg chl*a* m^{-3} and 1.4 ± 0.2 mg chl*a* m^{-3}, respectively) and occurred later in the season (June) (Table 2, Fig. 7a,b). Stations with shallow mixed layers (median < 25 m) and a higher stratification index (median SI > 5 x 10^3 kg m^{-4}) (Fig. 7c,d), also had relatively high average biomass in terms of carbon and chlorophyll *a* (Fig. 7a,b, Table 2). Low salinity waters (median < 33), found on the shelf (particularly Clusters 1 and 6) contributed to the shallow mixed layer depths (median < 20 m) and high stratification levels observed (i.e. haline stratification, median SI > 14x 10^3 kg m^{-4}), whereas relatively high sea surface temperature in June (> 4°C) in the central region of the Labrador Sea induced stratification (median SI from 6.0 to 8.0 x 10^3 kg m^{-4}, Clusters 2 and 4) and shoaled the mixed layer (i.e. thermal stratification, median mixed layer depths < 25 m) (Table 2).

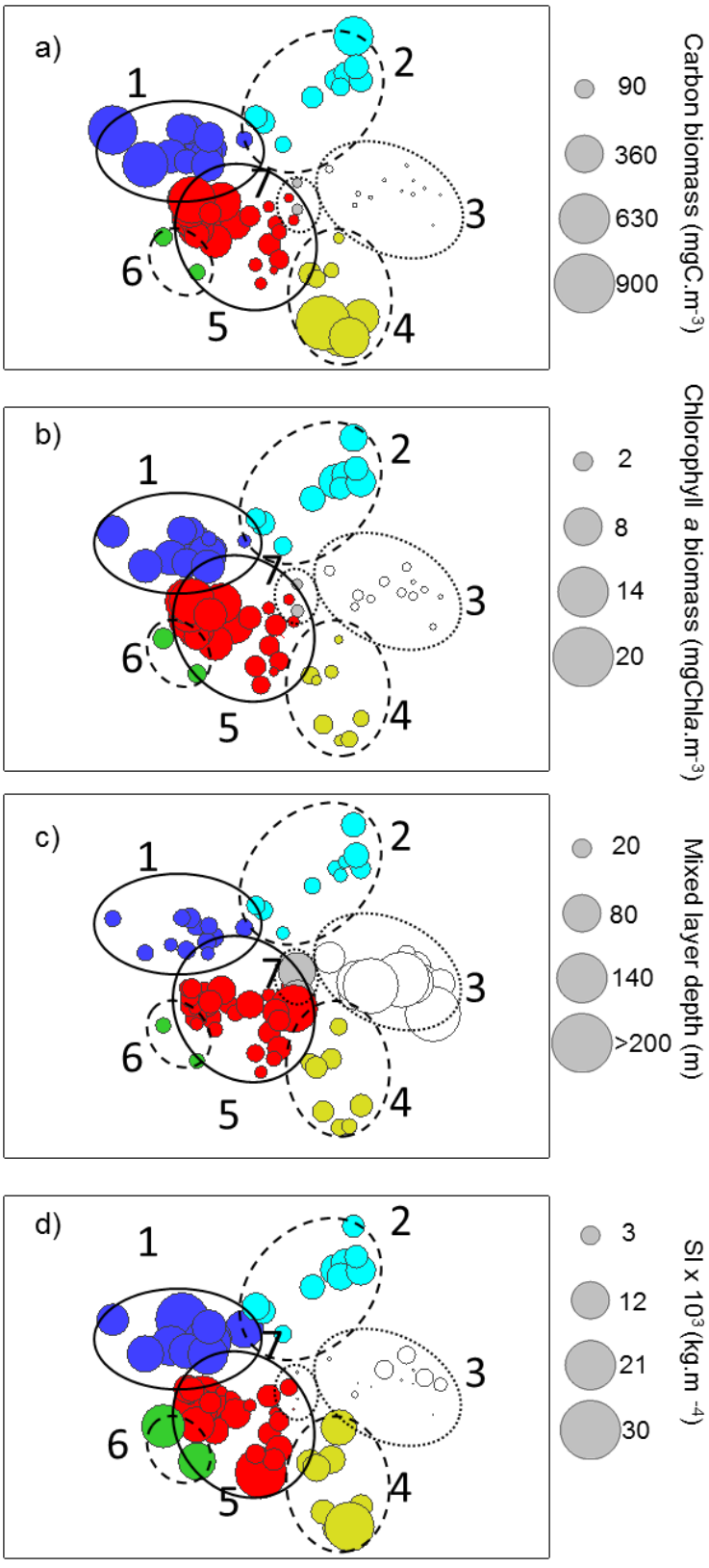

Figure 7. Bubble plots derived from nMDS (see Figure 5a) representing the average values (upper 50 m) of biomass in terms of (a) carbon, (b) chlorophyll *a*, (c) mixed layer depths (MLD), and (d) Stratification Index (SI x 10^{-3} kg m^{-4}) for the upper 60 m for each station. Filled colours refer to Cluster groups given in Figure 5a. Outlines around each Cluster represent the similarity in phytoplankton community structure within samples at 46% similarity level from samples collected during May and June (solid line), May only (dotted line) or June only (dashed line).

4. Discussion

4.1 Influence of Arctic and Atlantic waters on phytoplankton species composition

Phytoplankton community structure in the Labrador Sea during spring and early summer (2011 - 2014) varied according to the hydrographic characteristics (temperature, salinity and nutrient concentrations) of the distinct water masses of Atlantic (Irminger Current and Subpolar Mode Water derived from the North Atlantic Current) and Arctic (Labrador or West Greenland Current) origin, as well as their modifications at different stages of transformation. Overall, Arctic/polar phytoplankton species were present in the shelf waters, where the influence of Arctic waters was greater, whereas Atlantic phytoplankton species dominated in the central Labrador Sea, with a greater contribution of Atlantic water.

Blooms on the Labrador Shelf were comprised of Arctic and sea-ice diatoms that were able to grow in cold (< 0°C) and relatively fresh waters (< 33) (Table 2). In our study, polar/Arcto-boreal diatoms, such as *Thalassiosira* spp. (particularly *T. hyalina*, *T. antarctica var. borealis*, *T. nordenskioeldii*, *T. gravida* and *T. constricta*, data not shown) and *Bacterosira bathyomphala* were predominant in this region, which is consistent with the strong Arctic water influence via the Labrador Current on the Labrador Shelf (von Quillfeldt, 2001, 2000; Degerlund and Eilertsen, 2009; Sergeeva et al., 2010). Local sea ice melting also influenced the composition of diatoms in this region. The polar, cold water coastal diatom *Porosira glacialis* (Pike et al., 2009), and the sea-ice associated *Fossula arctica* and *Fragilariopsis* species (particularly *F. cylindrus* and *F. oceanica*; Caissie et al., 2010) were

abundant in both shelf regions, particularly on the Labrador Shelf, where sea ice melts during spring.

Polar diatom species, including *Thalassiosira* spp. (particularly *T. gravida*, *T. nordenskioeldii*, *T. antarctica var. borealis* and *T. hyalina*), *P. glacialis* and *C. socialis*, in addition to Atlantic species (*Rhizosolenia hebetata* f. *semispina*), were also observed on and near the Greenland shelf, suggesting that these waters were a mixture of Arctic and Atlantic origin - a characteristic typical of waters off the West Greenland Current (De Sève, 1999). Nonetheless, phytoplankton community structure differed from the Labrador Shelf, as the boreal prymnesiophyte *Phaeocystis pouchetii* was predominant in the eastern Labrador Sea (on and nearby the Greenland Shelf) during all study years, but was rarely observed on the Labrador Shelf. The reoccurring presence of *P. pouchetii* blooms in the central-eastern part of the Labrador Sea during spring is well-documented (Head et al., 2000; Stuart et al., 2000; Harrison et al., 2013; this study), suggesting that conditions in these waters are suitable for *P. pouchetii* growth every year (discussed below). *Pseudo-nitzschia granii*, a small needle-shaped diatom also observed in the eastern section of the Labrador Sea, had its distribution tightly linked to *P. pouchetii*, whose colony colonization by the diatom species has been previously reported in Norwegian waters (Hasle and Heimdal, 1998; Sazhin et al., 2007). High abundances of *Chaetoceros socialis* (herein referred to as Cluster 6) could potentially have followed blooms of *P. pouchetii* and diatoms on the west Greenland Shelf. *Chaetoceros socialis* has frequently been found during the later stages of blooms in Arctic waters (e.g. Baffin Bay, von Quillfeldt, 2000), where they can grow at relatively low nutrient concentrations (particularly silicate) because of their small cell size (< 10 μm) and lightly silicified cell walls (Booth et al., 2002).

The diatom *Ephemera planamembranaceae* was the most abundant species in offshore blooms observed in the central and central-western part of the Labrador Sea during

June 2012 and 2014 (Fig. 5). This species, typically reported in high numbers in the North Atlantic (Semina, 1997; Barnard et al., 2004), has been previously associated with shallow mixed layers and relatively high nutrient concentrations (Yallop, 2001); similar to conditions found in this study (Fig. 6, Table 2). *Fragilariopsis atlantica* co-dominated with *E. planamembranacea* in the central Labrador Sea. Unlike *F. cylindrus* and *F. oceanica*, *F. atlantica* is not found in sea-ice, being restricted to the water column and is mainly found in the Northern Atlantic Ocean (Lundholm and Hasle, 2010). The centric diatom *Rhizosolenia hebetata f. semispina*, also a representative North Atlantic diatom, formed blooms in the central eastern portion of the Labrador Sea in the summer of 2014 (Fig. 5). High numbers of *Rhizosolenia hebetata f. semispina* were found in association with large (subgenus *Phaeoceros, Thalassiostrix longissima*) and medium-sized diatoms (eg. *Chaetoceros decipiens*) in our study and have been previously observed in Norwegian waters (Hegseth and Sundfjord, 2008).

4.2 Environmental controls on Phaeocystis versus diatoms

In our study, all phytoplankton blooms were found in shallow mixed layers (median depth < 25 m) and stratified waters (median SI = 1 x 10^3 kg m^{-4}) (Table 2). However, during May 2014 a *P. pouchetii* bloom occurred in the eastern section of the Labrador Sea prior to the development of other phytoplankton blooms in the region. These *P. pouchetii* blooms were found in deeper mixed layers (~ 50 m) than in other years (data not shown). While low irradiances are not required for *Phaeocystis* growth, given that it can also be found in shallow mixed layers (Fragoso, 2009; Fragoso and Smith, 2012), the ability to grow under low light levels may confer on this species an advantage compared to larger diatoms. *P. pouchetii* blooms have also been reported to occur earlier in the season (April) due to the earlier haline-

650 driven stratification (Head et al., 2000; Frajka-Williams et al., 2009; Frajka-Williams and
651 Rhines, 2010), when light levels are lower than in May or June and the mixed layer is still
652 deep (< 100 m, Harrison et al., 2013).

653 Laboratory findings have also confirmed the ability of the southern ocean *Phaeocystis*
654 species (*P. antarctica*) to grow faster and increase their photosynthetic efficiency under
655 dynamic light intensities, typically found in deeper mixed layers (Kropuenske et al., 2009,
656 2010; Arrigo et al., 2010; Mills et al., 2010). Because of their ability to grow under variable
657 light, it is possible that *P. pouchetii* could grow and outcompete with diatoms while the
658 mixed lay depth shoals. As opposed to *P. pouchetii*, which is able to thrive under low light
659 intensities, sea-ice diatoms (such as *F. cylindrus*) invest heavily in photoprotective
660 mechanisms. This allows them to better adapt to higher light intensities, which are typically
661 found in shallow mixed layers (Kropuenske et al., 2009, 2010; Arrigo et al., 2010; Mills et
662 al., 2010) as well as late spring sea ice.

663 Nutrient resource competition has been suggested as one possible explanation for the
664 spatial segregation of *Phaeocystis pouchetii* and diatom blooms in the Labrador Sea
665 (Harrison and Li, 2008; Harrison et al., 2013) and elsewhere (Jiang et al., 2014). In our study,
666 cylinder or ribbon-shaped chain diatoms (i.e. *Thalassiosira* spp., *Bacterosira bathyomphala*
667 and *Fragilariopsis cylindrus*) dominated the Labrador Shelf waters. Such waters had only
668 slightly higher Si* values compared to the Greenland Shelf (Cluster 1 compared to Cluster 5,
669 see Table 2). Nonetheless, climatological studies show that the Labrador Shelf has a surplus
670 of silicate (silicate minus nitrate, Si* > 0) in the upper 150 m that decreases eastward, which
671 might explain the high number of diatoms in the west (Harrison et al., 2013). In this study, a
672 nitrate surplus of deep waters (~ 200 m) was evident across Labrador Sea shelves and basin
673 (negative Si*); however, the Labrador Shelf and Slope had a higher surplus of silicate in deep
674 waters compared to the central eastern section of the Labrador Sea (Fig. 3k,l). Hence, the

675 availability of silicate in waters of the Labrador Shelf might influence the dominance of
676 diatoms in this region as *P. pouchetii* does not require silicate, which could also be an
677 explanation for the east-west taxonomic segregation. Silicate depletion, however, is not a
678 necessary condition for *P. pouchetii* blooms, since it can co-dominate with diatoms when
679 silicate is not limiting. Jiang et al. (2014) argued that, under conditions where *P. pouchetii* is
680 dominant or co-dominant in a bloom, a sufficiently high pre-bloom concentration of nitrate (~
681 8 μM for the Massachusetts Bay) is needed (irrespective of the Si:N ratio). This would allow
682 more time for this species to grow, given that *Phaeocystis* grows slower than diatoms (Jiang
683 et al., 2014). Uptake rates of oxidised and reduced forms of nitrogen have also been
684 considered as an explanation for contrasting *Phaeocystis* and diatom-dominated blooms in
685 the North Sea, where *Phaeocystis* has been reported to have greater advantage due to
686 ammonium uptake compared with diatoms (Tungaraza et al., 2003). Ammonium
687 concentration was greater in the central-eastern part of the Labrador Sea in this study (Fig.
688 3h), particularly in the Greenland Shelf and Slope during June, which could also have
689 favoured the formation of *P. pouchetii* blooms in these waters.

690 *Phaeocystis* sp. colonies can control their buoyancy in the water column as a function
691 of light levels (positive buoyancy under light conditions, Wang and Tang, 2010), which could
692 also confer an advantage when accessing nutrients. In our study, *P. pouchetii* blooms on the
693 Greenland Shelf were concentrated in the subsurface and sometimes below the mixed layer,
694 being distributed within the upper 50 m, contrary to the diatom bloom on the Labrador Shelf
695 which was restricted to the upper mixed layer (< 25 m) (Fig 8 and 9, supplemental material).
696 Similar to the results presented here, *Phaeocystis pouchetii* blooms have also been reported to
697 be concentrated in subsurface waters around Greenland (Waniek et al., 2005; Frajka-
698 Williams and Rhines, 2010) and are capable of reaching deeper waters in the Fram Strait (>
699 75 m in Vogt et al., 2012b).

Phaeocystis colonies may also be able to proliferate because of their ability to escape predation by size mismatch (Jakobsen and Tang, 2002; Tang, 2003), unpalatable and toxic substances production (Aanesen et al., 1998; Dutz et al., 2005) and poor nutritional value of their colony matrix (Tang et al., 2001). In the eastern region of the central Labrador Sea basin and in the Greenland slope and shelf regions, the copepod *Calanus finmarchicus* is abundant in May-July (> 70,000 m^{-2}, 0-100 m, Head et al., 2003, 2013), where it dominates the biomass and is the most important grazer. Reports in the literature are somewhat contradictory as to whether *Phaeocystis* is a good food source for *Calanus* (see review by Nejstgaard et al., 2007), but most studies have been carried out with copepods and *Phaeocystis* from waters east of Greenland. In the northwest Atlantic, however, filtration rates for a mixed-species *Calanus* population from the Newfoundland Shelf were ~2.5 lower when they were feeding on natural seawater containing mainly *Phaeocystis* compared with when they were feeding on seawater that had a similar overall chlorophyll *a* concentration but contained a mixture of diatoms (Head and Harris, 1996).

4.4 Mixed layer depth, vertical stability and bloom development

Many studies of phytoplankton dynamics in the Labrador Sea have focused on how physical factors control the onset of the spring phytoplankton bloom (Wu et al., 2008a; Frajka-Williams et al., 2009; Frajka-Williams and Rhines, 2010; Lacour et al., 2015) . In our study, spring blooms in the Labrador Sea, irrespective of the hydrographic zone, occurred mostly in shallow mixed layers and areas of enhanced upper water column stratification, which suggests that vertical stability plays an important role in bloom development and maintenance. A similar observation was found by Wu et al. (2008a), who combined satellite-derived chlorophyll and historical data in modelling studies to confirm that mixed layer depth

724 plays a critical role in initiating the spring bloom in the Labrador Sea. While blooms
725 occurring in and near the shelf regions were due to haline-driven stratification, thermal-
726 stratification promoted blooms offshore, in the central Labrador Sea, as has been previously
727 observed (Wu et al., 2008; Frajka-Williams et al., 2009; Head et al., 2013).

728 Blooms have been reported to occur earlier along the eastern margin of the central
729 basin, and/or on the Greenland shelf because of the relatively shallow winter mixed layer
730 depth driven by haline stratification compared to the deep central basin (Frajka-Williams et
731 al., 2009; Head et al., 2013). A more recent study using calculated mixed layer
732 Photosynthetically Active Radiation (PAR) from Argo-floats and satellite observations
733 showed that the mean PAR levels within the mixed layer (~ 2.5 mol photons m^{-2} d^{-1}) is the
734 same during the initiation of the haline-driven bloom near the Greenland Shelf as it is in the
735 thermal driven bloom occurring in the central Labrador Sea, which starts one month later
736 (Lacour et al., 2015). Although mean PAR values were not measured *in situ* but estimated
737 from satellite and Argo-float observations, Lacour et al. (2015) concluded that increased light
738 availability, driven by either thermal or haline stratification, seems to be strongly linked to
739 bloom onset in the Labrador Sea. On the Labrador Shelf, shoaling of the mixed layer,
740 resulting from melting ice, has previously been established as a major trigger of diatom
741 blooms (Wu et al., 2007). However, in spite of a lack of sea ice on the Labrador shelf in May
742 2014, which could be an indication of sea ice melting, the mixed layer remained deep (~ 60
743 m), possibly due to strong winds.

744

745 **5- Conclusion**

746 In this study we have shown that phytoplankton community structure from the
747 Labrador Sea during spring and early summer of 2011 - 2014 varied according to the major

748 hydrographic features (temperature, salinity and nutrient concentrations) of distinct water
749 masses of Atlantic (Irminger Current), Arctic via Davis Strait (Labrador Current) or Arctic
750 via Denmark Strait (West Greenland Current) origin. In spite of interannual variations, which
751 in this study are difficult to assess because of the different sampling periods among years and
752 short duration of analysed records, phytoplankton community structure in the Labrador Sea
753 spring blooms had remarkably similar spatial and temporal patterns across the four years of
754 sampling. Arctic/polar large (> 50 μm) diatoms dominated the blooms in the inshore branch
755 of the LC, which were most influenced by Arctic and sea ice melt waters. *P. pouchetii* co-
756 dominated with diatoms (*Pseudo-nitzschia granii*, *Thalassiosira* spp.) at the interface of the
757 Arctic (WGC) and Atlantic (IC) waters. *Ephemera planamembranacea*, *Rhizosolenia*
758 *hebetata f. semispina* and *Fragilariopsis atlantica* were the main species found in offshore
759 waters of the central basin, which is strongly influenced by Atlantic waters. Lower salinities
760 and temperatures were associated with the Arctic/polar species found in the shelf waters with
761 higher influence of the Arctic outflow. Pre-bloom Si* (Si* from deeper waters), which were
762 comparatively higher on the Labrador Shelf and Slopes, might have influenced the taxonomic
763 segregation of polar diatoms dominating the west and *P. pouchetii* dominating the eastern
764 blooms. Nonetheless, the reason why *P. pouchetii* forms large blooms in the central-eastern
765 region of the Labrador Sea remains unclear.

766 In this study, shelf blooms occurred due to haline-driven stratification, whereas the
767 central basin bloom occurred later (June), when higher surface temperatures promoted
768 vertical stability. All blooms were found in shallow mixed layers (< 40 m) and more stratified
769 waters, which confirms that vertical stability plays an important role in bloom development
770 across the Labrador Sea. However, *Phaeocystis pouchetii* blooms were found in May 2014,
771 when the mixed layer was deeper (median = 75 m). This confirms the ability of *P. pouchetii*

to grow in deeper mixing layers, whereas Arctic/sea-ice diatom blooms were only found in shallower mixed layers (< 25 m).

6- Acknowledgements

We would like to thank Sinhue Torres-Valdes and Brian King (National Oceanography Centre) for providing the nutrient and hydrographic data from JR302 cruise and Elaine Mitchell (The Scottish Association for Marine Science) for guidance on Arctic phytoplankton taxonomy. Many thanks to Jeff Anning and Glen Harrison (Bedford Institute of Oceanography) for collecting the Lugols samples. The officers and crew of the *CCGS Hudson* and *RSS James Clark Ross* and the support of technicians and scientists from all cruises in analysing and providing the nutrient, chlorophyll and hydrographic data are also acknowledged. We are grateful to three reviewers who offered useful suggestions to improve the manuscript. G.M.F. was funded by a Brazilian PhD studentship, Science without Borders (CNPq, 201449/2012-9). This research was also partially funded by UK Ocean Acidification, a National Environment Research Council grant (NE/H017097/1) through an added value award.

7- References

Aanesen, R.T., Eilertsen, H.C., Stabell, O.B., 1998. Light-induced toxic properties of the marine alga *Phaeocystis pouchetii* towards cod larvae. Aquat. Toxicol. 40, 109–121.

Acevedo-Trejos, E., Brandt, G., Merico, A., Smith, S.L., 2013. Biogeographical patterns of phytoplankton community size structure in the oceans. Glob. Ecol. Biogeogr. 22, 1060–1070. doi:10.1111/geb.12071

Anisimov, O.A., Vaughan, D.G., Callaghan, T. V., Furgal, C., Marchant, H., Prowse, T.D., Vilhjálmsson, H., Walsh, J.E., Fitzharris, B., Zealand, N.E.W., Canada, T.P., Uk, D.G.V., 2007. Polar Regions (Arctic and Antarctic). Clim. Chang. 15, 653–685.

798 Ardyna, M., Babin, M., Gosselin, M., Devred, E., Rainville, L., Tremblay, J.-É., 2014. Recent Arctic
799 Ocean sea-ice loss triggers novel fall phytoplankton blooms. Geophys. Res. Lett. 41, 6207–6212.
800 doi:10.1002/2014GL061047
801 Arrigo, K.R., Mills, M.M., Kropuenske, L.R., Van Dijken, G.L., Alderkamp, A.C., Robinson, D.H., 2010.
802 Photophysiology in two major southern ocean phytoplankton taxa: Photosynthesis and growth
803 of *Phaeocystis antarctica* and *Fragilariopsis cylindrus* under different irradiance levels. Integr.
804 Comp. Biol. 50, 950–966. doi:10.1093/icb/icq021
805 Arrigo, K.R., van Dijken, G., Pabi, S., 2008. Impact of a shrinking Arctic ice cover on marine primary
806 production. Geophys. Res. Lett. 35, L19603. doi:10.1029/2008GL035028
807 Barnard, R., Batten, S.D., Beaugrand, G., Buckland, C., Conway, D.V.P., Edwards, M., Finlayson, J.,
808 Gregory, L.W., Halliday, N.C., John, A.W.G., Johns, D.G., Johnson, A.D., Jonas, T.D., Lindley, J.A.,
809 Nyman, J., Pritchard, P., Reid, P.C., Richardson, A.J., Saxby, R.E., Sidey, J., Smith, M.A., Stevens,
810 D.P., Taylor, C.M., Tranter, P.R.G., Walne, A.W., Wootton, M., Wotton, C.O.M., Wright, J.C.,
811 2004. Continuous plankton records: Plankton Atlas of the north Atlantic Ocean (1958-1999). II.
812 Biogeographical charts. Mar. Ecol. Prog. Ser. doi:10.3554/mepscpr011
813 Bhatia, M.P., Kujawinski, E.B., Das, S.B., Breier, C.F., Henderson, P.B., Charette, M.A., 2013.
814 Greenland meltwater as a significant and potentially bioavailable source of iron to the ocean.
815 Nat. Geosci. 6, 274–278. doi:10.1038/ngeo1746
816 Booth, B.C., Larouche, P., Bélanger, S., Klein, B., Amiel, D., Mei, Z.P., 2002. Dynamics of *Chaetoceros*
817 *socialis* blooms in the North Water. Deep. Res. Part II Top. Stud. Oceanogr. 49, 5003–5025.
818 doi:10.1016/S0967-0645(02)00175-3
819 Brun, P., Vogt, M., Payne, M.R., Gruber, N., O'Brien, C.J., Buitenhuis, E.T., Le Quéré, C., Leblanc, K.,
820 Luo, Y.-W., 2015. Ecological niches of open ocean phytoplankton taxa. Limnol. Oceanogr. n/a–
821 n/a. doi:10.1002/lno.10074
822 Caissie, B.E., Brigham-Grette, J., Lawrence, K.T., Herbert, T.D., Cook, M.S., 2010. Last Glacial
823 Maximum to Holocene sea surface conditions at Umnak Plateau, Bering Sea, as inferred from
824 diatom, alkenone, and stable isotope records. Paleoceanography. doi:10.1029/2008PA001671
825 Clarke, K.R., 1993. Non-parametric multivariate analyses of changes in community structure. Austr. J.
826 Ecol. 18, 117–143. doi:10.1111/j.1442-9993.1993.tb00438.x
827 Clarke, K.R., Warwick, R.M., 2001. Change in marine communities: an approach to statistical analysis
828 and interpretation, 2nd Editio. ed. PRIMER-E, Plymouth.
829 Collos, Y., 2002. Determination of particulate carbon and nitrogen in coastal waters., in: Subba Rao
830 DV (Ed.), Pelagic Ecology Methodology. A. A. Balkema Publishers, Tokyo, pp. 333–341.
831 Cota, G.F., 2003. Bio-optical properties of the Labrador Sea. J. Geophys. Res.
832 doi:10.1029/2000JC000597
833 De Sève, M.A., 1999. Transfer function between surface sediment diatom assemblages and sea-
834 surface temperature and salinity of the Labrador Sea. Mar. Micropaleontol. 36, 249–267.
835 doi:10.1016/S0377-8398(99)00005-5
836 Degerlund, M., Eilertsen, H.C., 2010. Main species characteristics of phytoplankton spring blooms in
837 NE Atlantic and Arctic waters (68-80^{o} N). Estuaries and Coasts 33, 242–269.
838 doi:10.1007/s12237-009-9167-7
839 DeGrandpre, M.D., Körtzinger, A., Send, U., Wallace, D.W.R., Bellerby, R.G.J., 2006. Uptake and
840 sequestration of atmospheric CO_2 in the Labrador Sea deep convection region. Geophys. Res.
841 Lett. 33, L21S03. doi:10.1029/2006GL026881
842 Dickson, B., Yashayaev, I., Meincke, J., Turrell, B., Dye, S., Holfort, J., 2002. Rapid freshening of the
843 deep North Atlantic Ocean over the past four decades. Nature 416, 832–837.
844 doi:10.1038/416832a
845 Dutz, J., Klein Breteler, W.C.M., Kramer, G., 2005. Inhibition of copepod feeding by exudates and
846 transparent exopolymer particles (TEP) derived from a *Phaeocystis globosa* dominated
847 phytoplankton community. Harmful Algae 4, 929–940.

Finkel, Z. V., Beardall, J., Flynn, K.J., Quigg, A., Rees, T.A. V., Raven, J.A., 2010. Phytoplankton in a changing world: Cell size and elemental stoichiometry. J. Plankton Res. doi:10.1093/plankt/fbp098

Fragoso, G.M., 2009. Hydrography and phytoplankton distribution in the Amundsen and Ross Seas. College of William and Mary.

Fragoso, G.M., Smith, W.O., 2012. Influence of hydrography on phytoplankton distribution in the Amundsen and Ross Seas, Antarctica. J. Mar. Syst. 89, 19–29. doi:10.1016/j.jmarsys.2011.07.008

Frajka-Williams, E., Rhines, P.B., 2010. Physical controls and interannual variability of the Labrador Sea spring phytoplankton bloom in distinct regions. Deep. Res. Part I Oceanogr. Res. Pap. 57, 541–552. doi:10.1016/j.dsr.2010.01.003

Frajka-Williams, E., Rhines, P.B., Eriksen, C.C., 2009. Physical controls and mesoscale variability in the Labrador Sea spring phytoplankton bloom observed by Seaglider. Deep. Res. Part I Oceanogr. Res. Pap. 56, 2144–2161. doi:10.1016/j.dsr.2009.07.008

Goes, J.I., Gomes, H.D.R., Chekalyuk, A.M., Carpenter, E.J., Montoya, J.P., Coles, V.J., Yager, P.L., Berelson, W.M., Capone, D.G., Foster, R. a., Steinberg, D.K., Subramaniam, A., Hafez, M. a., 2014. Influence of the Amazon River discharge on the biogeography of phytoplankton communities in the western tropical north Atlantic. Prog. Oceanogr. 120, 29–40. doi:10.1016/j.pocean.2013.07.010

Hall, M.M., Torres, D.J., Yashayaev, I., 2013. Absolute velocity along the AR7W section in the Labrador Sea. Deep. Res. Part I Oceanogr. Res. Pap. 72, 72–87. doi:10.1016/j.dsr.2012.11.005

Harrison, G.W., Yngve Børsheim, K., Li, W.K.W., Maillet, G.L., Pepin, P., Sakshaug, E., Skogen, M.D., Yeats, P.A., 2013. Phytoplankton production and growth regulation in the Subarctic North Atlantic: A comparative study of the Labrador Sea-Labrador/Newfoundland shelves and Barents/Norwegian/Greenland seas and shelves. Prog. Oceanogr. 114, 26–45. doi:10.1016/j.pocean.2013.05.003

Harrison, W., Li, W., 2008. Phytoplankton growth and regulation in the Labrador Sea: light and nutrient limitation. J. Northwest Atl. Fish. Sci. doi:10.2960/J.v39.m592

Hasle, G.R., Heimdal, B.R., 1998. The net phytoplankton in Kongsfjorden, Svalbard, July 1988, with general remarks on species composition of Arctic phytoplankton. Polar Res. 17, 31–52. doi:10.1111/j.1751-8369.1998.tb00257.x

Head, E.J.H., Harris, L.R., 1996. Chlorophyll destruction by *Calanus* spp. grazing on phytoplankton: Kinetics, effects of ingestion rate and feeding history, and a mechanistic interpretation. Mar. Ecol. Prog. Ser. 135, 223–235. doi:10.3354/meps135223

Head, E.J.H., Harris, L.R., Campbell, R.W., 2000. Investigations on the ecology of *Calanus* spp. in the Labrador Sea. I. Relationship between the phytoplankton bloom and reproduction and development of *Calanus finmarchicus* in spring. Mar. Ecol. Prog. Ser. 193, 53–73. doi:10.3354/meps193053

Head, E.J.H., Harris, L.R., Yashayaev, I., 2003. Distributions of *Calanus* spp. and other mesozooplankton in the Labrador Sea in relation to hydrography in spring and summer (1995-2000). Prog. Oceanogr. doi:10.1016/S0079-6611(03)00111-3

Head, E.J.H., Melle, W., Pepin, P., Bagøien, E., Broms, C., 2013. On the ecology of *Calanus finmarchicus* in the Subarctic North Atlantic: A comparison of population dynamics and environmental conditions in areas of the Labrador Sea-Labrador/Newfoundland Shelf and Norwegian Sea Atlantic and Coastal Waters. Prog. Oceanogr. 114, 46–63. doi:10.1016/j.pocean.2013.05.004

Hegseth, E.N., Sundfjord, A., 2008. Intrusion and blooming of Atlantic phytoplankton species in the high Arctic. J. Mar. Syst. 74, 108–119. doi:10.1016/j.jmarsys.2007.11.011

Henson, S. a., Dunne, J.P., Sarmiento, J.L., 2009. Decadal variability in North Atlantic phytoplankton blooms. J. Geophys. Res. Ocean. 114, 1–11. doi:10.1029/2008JC005139

898 Holm-Hansen, O., Lorenzen, C.J., Holmes, R.W., Strickland, J.D.H., 1965. Fluorometric Determination
899 of Chlorophyll. ICES J. Mar. Sci. 30, 3–15. doi:10.1093/icesjms/30.1.3
900 Jakobsen, H.H., Tang, K.W., 2002. Effects of protozoan grazing on colony formation in Phaeocystis
901 globosa (Prymnesiophyceae) and the potential costs and benefits 27, 261–273.
902 Jiang, M., Borkman, D.G., Scott Libby, P., Townsend, D.W., Zhou, M., 2014. Nutrient input and the
903 competition between *Phaeocystis pouchetii* and diatoms in Massachusetts Bay spring bloom. J.
904 Mar. Syst. 134, 29–44. doi:10.1016/j.jmarsys.2014.02.011
905 Kahru, M., Brotas, V., Manzano-Sarabia, M., Mitchell, B.G., 2011. Are phytoplankton blooms
906 occurring earlier in the Arctic? Glob. Chang. Biol. 17, 1733–1739. doi:10.1111/j.1365-
907 2486.2010.02312.x
908 Kerouel, R., Aminot, a, 1997. Fluorometric determination of ammonia in sea and estuarine water by
909 direct segmented flow analysis. Mar. Chem. 57, 265–275.
910 Kieke, D., Yashayaev, I., 2015. Studies of Labrador Sea Water formation and variability in the
911 subpolar North Atlantic in the light of international partnership and collaboration. Prog.
912 Oceanogr. 132, 220–232. doi:10.1016/j.pocean.2014.12.010
913 Kropuenske, L.R., Mills, M.M., Van Dijken, G.L., Alderkamp, A.C., Mine Berg, G., Robinson, D.H.,
914 Welschmeyer, N.A., Arrigo, K.R., 2010. Strategies and rates of photoacclimation in two major
915 southern ocean phytoplankton taxa: *Phaeocystis antarctica* (haptophyta) and *Fragilariopsis*
916 *cylindrus* (bacillariophyceae). J. Phycol. 46, 1138–1151. doi:10.1111/j.1529-8817.2010.00922.x
917 Kropuenske, L.R., Mills, M.M., van Dijken, G.L., Bailey, S., Robinson, D.H., Welschmeyer, N.A., Arrigo,
918 K.R., 2009. Photophysiology in two major Southern Ocean phytoplankton taxa: Photoprotection
919 in *Phaeocystis antarctica* and *Fragilariopsis cylindrus* . Limnol. Oceanogr. 54, 1176–1196.
920 doi:10.4319/lo.2009.54.4.1176
921 Lacour, L., Claustre, H., Prieur, L., Ortenzio, F.D., 2015. Phytoplankton biomass cycles in the North
922 Atlantic subpolar gyre: A similar mechanism for two different blooms in the Labrador Sea
923 5403–5410. doi:10.1002/2015GL064540.Received
924 Lepš, J., Šmilauer, P., 2003. Multivariate analysis of ecological data using CANOCO. Cambridge
925 university press.
926 Litchman, E., Edwards, K.F., Klausmeier, C. a., Thomas, M.K., 2012. Phytoplankton niches, traits and
927 eco-evolutionary responses to global environmental change. Mar. Ecol. Prog. Ser. 470, 235–
928 248. doi:10.3354/meps09912
929 Lundholm, N., Hasle, G.R., 2010. *Fragilariopsis* (Bacillariophyceae) of the Northern Hemisphere –
930 morphology, taxonomy, phylogeny and distribution, with a description of F. pacifica sp. nov.
931 Phycologia. doi:10.2216/09-97.1
932 Martz, T.R., DeGrandpre, M.D., Strutton, P.G., McGillis, W.R., Drennan, W.M., 2009. Sea surface
933 pCO_2 and carbon export during the Labrador Sea spring-summer bloom: An in situ mass
934 balance approach. J. Geophys. Res. 114, C09008. doi:10.1029/2008JC005060
935 Mathot, S., Smith, W.O., Carlson, C.A., Garrison, D.L., Gowing, M.M., Vickers, C.L., 2000. Carbon
936 partitioning within *Phaeocystis antarctica* (prymnesiophyceae) colonies in the Ross sea,
937 Antarctica. J. Phycol. 36, 1049–1056. doi:10.1046/j.1529-8817.2000.99078.x
938 Medlin, L.K., Priddle, J., 1990. Polar marine diatoms. British Antarctic Survey, Cambridge.
939 Menden-Deuer, S., Lessard, E.J., 2000. Carbon to volume relationships for dinoflagellates, diatoms,
940 and other protist plankton. Limnol. Oceanogr. 45, 569–579. doi:10.4319/lo.2000.45.3.0569
941 Mills, M.M., Kropuenske, L.R., Van Dijken, G.L., Alderkamp, A.C., Berg, G.M., Robinson, D.H.,
942 Welschmeyer, N.A., Arrigo, K.R., 2010. Photophysiology in two southern ocean phytoplankton
943 taxa: Photosynthesis of *Phaeocystis antarctica* (prymnesiophyceae) and *Fragilariopsis cylindrus*
944 (bacillariophyceae) under simulated mixed-layer irradiance. J. Phycol. 46, 1114–1127.
945 doi:10.1111/j.1529-8817.2010.00923.x
946 Montagnes, D.J.S., Franklin, D.J., 2001. Effect of temperature on diatom volume, growth rate, and
947 carbon and nitrogen content: Reconsidering some paradigms. Limnol. Oceanogr. 46, 2008–
948 2018. doi:10.4319/lo.2001.46.8.2008

949 Montes-Hugo, M., Doney, S.C., Ducklow, H.W., Fraser, W., Martinson, D., Stammerjohn, S.E.,
950 Schofield, O., 2009. Recent Changes in Phytoplankton Western Antarctic Peninsula. Science
951 (80-.). 323, 1470–1473.
952 Nejstgaard, J.C., Tang, K.W., Steinke, M., Dutz, J., Koski, M., Antajan, E., Long, J.D., 2007. Zooplankton
953 grazing on *Phaeocystis* : A quantitative review and future challenges. Biogeochemistry 83,
954 147–172. doi:10.1007/s10533-007-9098-y
955 Olenina, I., Hajdu, S., Edler, L., Andersson, A., Wasmund, N., Busch, S., Göbel, J., Gromisz, S., Huseby,
956 S., Huttunen, M., Jaanus, A., Kokkonen, P., Ledaine, I., Niemkiewicz, E., 2006. Biovolumes and
957 size-classes of phytoplankton in the Baltic Sea. HELCOM Balt.Sea Environ. Proc. No. 106.
958 Pabi, S., van Dijken, G.L., Arrigo, K.R., 2008. Primary production in the Arctic Ocean, 1998–2006. J.
959 Geophys. Res. 113, C08005. doi:10.1029/2007JC004578
960 Peterson, T.D., Toews, H.N.J., Robinson, C.L.K., Harrison, P.J., 2007. Nutrient and phytoplankton
961 dynamics in the Queen Charlotte Islands (Canada) during the summer upwelling seasons of
962 2001-2002. J. Plankton Res. 29, 219–239. doi:10.1093/plankt/fbm010
963 Pike, J., Crosta, X., Maddison, E.J., Stickley, C.E., Denis, D., Barbara, L., Renssen, H., 2009.
964 Observations on the relationship between the Antarctic coastal diatoms *Thalassiosira*
965 *antarctica* Comber and *Porosira glacialis* (Grunow) Jørgensen and sea ice concentrations during
966 the late Quaternary. Mar. Micropaleontol. 73, 14–25. doi:10.1016/j.marmicro.2009.06.005
967 Rousseau, V., Mathot, S., Lancelot, C., 1990. Calculating carbon biomass of *Phaeocystis* sp. from
968 microscopic observations. Mar. Biol. 107, 305–314. doi:10.1007/BF01319830
969 Sazhin, A.F., Artigas, L.F., Nejstgaard, J.C., Frischer, M.E., 2007. The colonization of two *Phaeocystis*
970 species (Prymnesiophyceae) by pennate diatoms and other protists: A significant contribution
971 to colony biomass, in: *Phaeocystis* , Major Link in the Biogeochemical Cycling of Climate-
972 Relevant Elements. pp. 137–145. doi:10.1007/978-1-4020-6214-8_11
973 Semina, H.J., 1997. An outline of the geographical distribution of oceanic phytoplankton., in: Blaxter,
974 G.H.S., Southward, A.G., Gebruck, A.V., Southwards, E.C., Tyler, P.A. (Eds.), Advances in Marine
975 Biology. Academic Press, London, pp. 527–563. doi:10.1016/S0065-2881(08)60020-6
976 Sergeeva, V.M., Sukhanova, I.N., Flint, M. V., Pautova, L.A., Grebmeier, J.M., Cooper, L.W., 2010.
977 Phytoplankton community in the Western Arctic in July–August 2003. Oceanology.
978 doi:10.1134/S0001437010020049
979 Solórzano, L., 1969. Determination of ammonia in natural waters by the phenol hypochlorite
980 method. Limnol. Oceanogr. 14, 799–801. doi:10.4319/lo.1969.14.5.0799
981 Straneo, F., Saucier, F., 2008. The outflow from Hudson Strait and its contribution to the Labrador
982 Current. Deep Sea Res. Part I Oceanogr. Res. Pap. 55, 926–946. doi:10.1016/j.dsr.2008.03.012
983 Strutton, P.G., Martz, T.R., DeGrandpre, M.D., McGillis, W.R., Drennan, W.M., Boss, E., 2011. Bio-
984 optical observations of the 2004 Labrador Sea phytoplankton bloom. J. Geophys. Res. 116,
985 C11037. doi:10.1029/2010JC006872
986 Stuart, V., Sathyendranath, S., Head, E.J.H., Platt, T., Irwin, B., Maass, H., 2000. Bio-optical
987 characteristics of diatom and prymnesiophyte populations in the Labrador Sea. Mar. Ecol. Prog.
988 Ser. 201, 91–106. doi:10.3354/meps201091
989 Sun, J., Liu, D., 2003. Geometric models for calculating cell biovolume and surface area for
990 phytoplankton. J. Plankton Res. 25, 1331–1346. doi:10.1093/plankt/fbg096
991 Tang, K.W., 2003. Grazing and colony size development in *Phaeocystis globosa* (Prymnesiophyceae):
992 the role of a chemical signal. J. Plankton Res. 25, 831–842.
993 Tang, K.W., Jakobsen, H.H., Visser, a. W., 2001. Phaeocystis globosa (Prymnesiophyceae) and the
994 planktonic food web: Feeding, growth, and trophic interactions among grazers. Limnol.
995 Oceanogr. 46, 1860–1870. doi:10.4319/lo.2001.46.8.1860
996 Throndsen, J., Hasle, G.R., Tangen, K., 2007. Phytoplankton of Norwegian coastal waters. Almater
997 Forlag AS.

Tian, R.C., Deibel, D., Rivkin, R.B., Vézina, A.F., 2004. Biogenic carbon and nitrogen export in a deep-convection region: Simulations in the Labrador Sea. Deep. Res. Part I Oceanogr. Res. Pap. 51, 413–437. doi:10.1016/j.dsr.2003.10.015

Tomas, C.R., 1997. Identifying marine phytoplankton. Academic press.

Tungaraza, C., Rousseau, V., Brion, N., Lancelot, C., Gichuki, J., Baeyens, W., Goeyens, L., 2003. Contrasting nitrogen uptake by diatom and Phaeocystis-dominated phytoplankton assemblages in the North Sea. J. Exp. Mar. Bio. Ecol. 292, 19–41. doi:10.1016/S0022-0981(03)00145-X

Utermöhl, H., 1958. Improvement of the quantitative methods for phytoplankton. Mitt. Int. Ver. Limnol. 9, 1–38.

Vogt, M., O'Brien, C., Peloquin, J., Schoemann, V., Breton, E., Estrada, M., Gibson, J., Karentz, D., Van Leeuwe, M.A., Stefels, J., Widdicombe, C., Peperzak, L., 2012. Global marine plankton functional type biomass distributions: *Phaeocystis* spp. Earth Syst. Sci. Data 4, 107–120. doi:10.5194/essd-4-107-2012

Von Quillfeldt, C., 2000. Common diatom species in Arctic spring blooms: their distribution and abundance. Bot. Mar. 43, 499–516. doi:10.1515/BOT.2000.050

Von Quillfeldt, C., 2001. Identification of some easily confused common diatom species in Arctic spring blooms. Bot. Mar. 44, 375–389. doi:10.1515/BOT.2001.048

Wang, X., Tang, K.W., 2010. Buoyancy regulation in *Phaeocystis globosa* Scherffel colonies. Open Mar. Biol. J. 4, 115–121.

Waniek, J., Holliday, N., Davidson, R., Brown, L., Henson, S., 2005. Freshwater control of onset and species composition of Greenland shelf spring bloom. Mar. Ecol. Prog. Ser. 288, 45–57. doi:10.3354/meps288045

Weller, R.A., Plueddemann, A.J., 1996. Observations of the vertical structure of the oceanic boundary layer. J. Geophys. Res. doi:10.1029/96JC00206

Wu, Y., Peterson, I.K., Tang, C.C.L., Platt, T., Sathyendranath, S., Fuentes-Yaco, C., 2007. The impact of sea ice on the initiation of the spring bloom on the Newfoundland and Labrador Shelves. J. Plankton Res. 29, 509–514. doi:10.1093/plankt/fbm035

Wu, Y., Platt, T., Tang, C., Sathyendranath, S., 2008. Regional differences in the timing of the spring bloom in the Labrador Sea. Mar. Ecol. Prog. Ser. 355, 9–20. doi:10.3354/meps07233

Wu, Y., Platt, T., Tang, C.C.L., Sathyendranath, S., Devred, E., Gu, S., 2008. A summer phytoplankton bloom triggered by high wind events in the Labrador Sea, July 2006. Geophys. Res. Lett. 35, L10606.

Yallop, M.L., 2001. Distribution patterns and biomass estimates of diatoms and autotrophic dinoflagellates in the NE Atlantic during June and July 1996. Deep. Res. Part II Top. Stud. Oceanogr. 48, 825–844. doi:10.1016/S0967-0645(00)00099-0

Yankovsky, A.E., Yashayaev, I., 2014. Surface buoyant plumes from melting icebergs in the Labrador Sea. Deep. Res. Part I Oceanogr. Res. Pap. 91, 1–9. doi:10.1016/j.dsr.2014.05.014

Yashayaev, I., 2007. Hydrographic changes in the Labrador Sea, 1960-2005. Prog. Oceanogr. 73, 242–276. doi:10.1016/j.pocean.2007.04.015

Yashayaev, I., Loder, J.W., 2009. Enhanced production of Labrador Sea Water in 2008. Geophys. Res. Lett. 36. doi:10.1029/2008GL036162

Yashayaev, I., Seidov, D., 2015. The role of the Atlantic Water in multidecadal ocean variability in the Nordic and Barents Seas. Prog. Oceanogr. 132, 68–127. doi:10.1016/j.pocean.2014.11.009

Yashayaev, I., Seidov, D., Demirov, E., 2015. A new collective view of oceanography of the Arctic and North Atlantic basins. Prog. Oceanogr. doi:10.1016/j.pocean.2014.12.012

Yebra, L., Harris, R.P., Head, E.J.H., Yashayaev, I., Harris, L.R., Hirst, A.G., 2009. Mesoscale physical variability affects zooplankton production in the Labrador Sea. Deep. Res. Part I Oceanogr. Res. Pap. 56, 703–715. doi:10.1016/j.dsr.2008.11.008